

Drew University

College of Liberal Arts

***Reactivity of  $Os_2(CO)_6(RCONH)_2$ : mechanisms and thermodynamic properties***

A Thesis in Chemistry

By

Sarah Costa

Examining Committee:

Mary-Ann Pearsall, Thesis Advisor

Chemistry

Alan Rosan, Member

Chemistry

Jim Supplee, Member

Physics

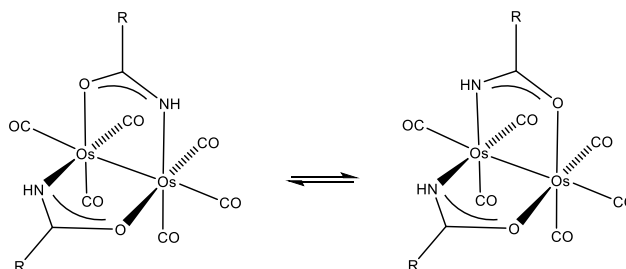
May 2019

## **Table of Content**

1. Abstract
2. Introduction
  - a. Types of Ligands on a Metal Complex
  - b. Organometallic complexes
  - c. Anti-Cancer Activity of Osmium Cluster and Analogs Species
  - d. Research on Reactivity of Osmium
  - e. Polymer
  - f. Previous Research with the Pearsall Group
3. Methods
  - a. Infrared Spectroscopy
  - b. Thin Layer Chromatography
  - c. Nuclear Magnetic Resonance Spectroscopy
  - d. Density Functional Theory Calculations
  - e. Microwave Synthesis
4. Experimental
  - a. Synthesis of the Acetamide-Polymer  $[\text{Os}_2(\text{CO})_4(\text{CH}_3\text{CONH})_2]_n$  in toluene at  $110^\circ\text{C}$
  - b. Reversal of the Acetamide-Polymer  $\text{Os}_2(\text{CO})_4(\text{CH}_3\text{CONH})_2$  in toluene at  $110^\circ\text{C}$  with  $\text{CO}(\text{g})$
  - c.  $\text{Os}_3(\text{CO})_{10}(\text{OEt})_2$  with Acetic Acid in Cyclohexane at  $80^\circ\text{C}$
  - d. Synthesis of the Acetic Acid-Polymer  $\text{Os}_2(\text{CO})_4(\text{OOCCH}_3)_2$  in toluene at  $110^\circ\text{C}$  and Reversal with  $\text{CO}(\text{g})$
  - e. Synthesis of  $\text{Os}_2(\text{CO})_6(\text{RCONH})_2$  using  $\text{Os}_3(\text{CO})_{10}(\text{OEt})_2$  and acetamide in toluene at  $110^\circ\text{C}$
  - f. Exchange of coordinated amide on  $\text{Os}_2(\text{CO})_6(\text{RCONH})_2$  with free carboxylic acid
  - g. Microwave reaction of  $\text{Os}_3(\text{CO})_{12}$  and benzamide
  - h. Microwave reaction of  $\text{Os}_3(\text{CO})_{10}(\text{OEt})_2$  with benzamide
5. Results and Discussion
  - a. Synthesis of  $\text{Os}_2(\text{CO})_6(\text{RCONH})_2$  and  $\text{Os}_2(\text{CO})_4(\text{RCONH})_2$ 
    - i. Acetamide monomer
    - ii.  $[\text{Os}_2(\text{CO})_4(\text{CH}_3\text{CONH})_2]_n$  Polymer
  - b. Thermodynamic analysis of  $\text{Os}_2(\text{CO})_6(\text{CH}_3\text{CONH})_2$
  - c. Microwave reaction of  $\text{Os}_3(\text{CO})_{10}(\text{OEt})_2$  with benzamide
6. Conclusion
7. Appendix
8. References

## Abstract

The osmium diamide carbonyl complexes  $\text{Os}_2(\text{CO})_6(\text{RCONH})_2$  ( $\text{R} = \text{CH}_3, \text{Ph}$ ) and the acetamide polymer,  $[\text{Os}_2(\text{CO})_4(\text{CH}_3\text{CONH})_2]_n$  were synthesized and investigated for their kinetic and thermodynamic properties.



The  $\text{Os}_2(\text{CO})_6(\text{RCONH})_2$  ( $\text{R} = \text{CH}_3, \text{Ph}$ ) monomers exist as two isomers in which the amides coordinate in a head-to-tail and head-to-head configuration. The interconversion of the isomers of  $\text{Os}_2(\text{CO})_6(\text{CH}_3\text{CONH})_2$  was investigated by  $^1\text{H}$  NMR over a range of temperatures to determine the thermodynamic parameters;  $\Delta S + 6.14 \text{ J}$  and  $\Delta H - 1.65 \text{ J}$ . The lack of exchange of the coordinated amide with a free carboxylic acid in solution proved the mechanism was intramolecular and the polymerization was more favorable than an exchange with the coordinated amide.

The proposed acetamide polymer structure,  $[\text{Os}_2(\text{CO})_4(\text{CH}_3\text{CONH})_2]_n$ , is bonded together by a weak osmium oxygen bond. In the presence of carbon monoxide, the polymer converted back to the monomer species as confirmed by IR. The analogous benzamide complex did not polymerize. Additionally, prolonged heating of the  $\text{Os}_2(\text{CO})_6(\text{COOCH}_3)_2$  complex led to a polymer formation, which decomposed to the monomer species over time.

## Introduction

As part of the Pearsall research group, I have investigated the products of the reaction of triosmiumdecarbonylbisethoxide, “bisethoxide”  $\text{Os}_3(\text{CO})_{10}(\text{OEt})_2$ , with amides. For the rest of this paper triosmiumdecarbonylbisethoxide will be referred to as Compound A. This reaction forms two isomers of the monomer product  $(\text{Os}_2(\text{CO})_6(\text{RCONH})_2)$  (Figure 1a). Isomer B is the product of the reaction with acetamide and Isomer C is the product with benzamide. The specific monomeric,  $(\text{Os}_2(\text{CO})_6(\text{RCONH})_2)$ , isomers will be referred to as the head-to-head isomer, and the head-to-tail isomer. A related polymer species, proposed to be  $[\text{Os}_2(\text{CO})_4(\text{RCONH})_2]_n$ , Compound D (Figure 1b).

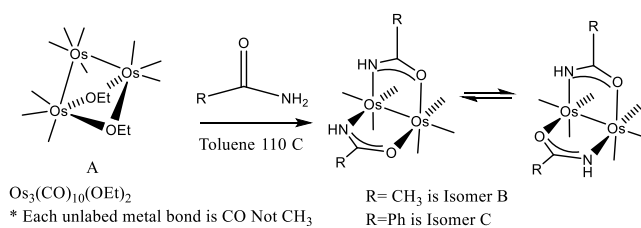


Figure 1a: Triosmiumdecarbonylbisethoxide reacting with an amide to synthesize a diosmium structure with cis bridged amide groups. There are two isomers of the product; a head-to-head (A) and a head-to-tail (B).

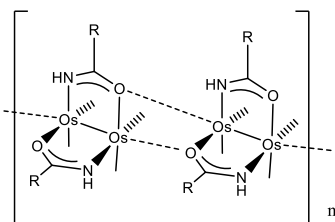


Figure 1b: Proposed structure of Compound D, the acetamide osmium polymer.

## Types of Ligands on a Metal Complex

There are three types of ligands associated with a metal complex:  $\sigma$ -donor,  $\pi$ -donor, and  $\pi$ -acceptor.  $\sigma$ -donor ligands only donate a  $\sigma$ -lone pair while  $\pi$ -donor ligands both donate  $\pi$

electrons and  $\sigma$ -electrons.<sup>1</sup> In addition, these proposed non-bonding orbitals that overlap donate electron density to the metal d-orbitals. Similarly,  $\pi$ -acceptor ligands donate a lone pair but have vacant and overlapping non-bonding orbitals that experience electron density donation from the metal d-orbital (Figure 2).

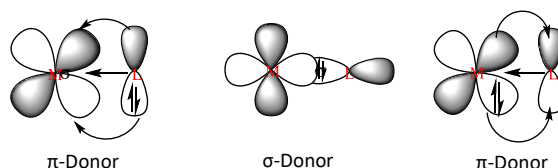


Figure 2: A visual description of types of ligands  $\pi$ -donor,  $\sigma$ -donor, and  $\pi$ -acceptor

### Organometallic complexes

Organometallic complexes are metal clusters containing a metal carbon bond. A transition metal carbonyl (CO) complex is a molecule containing both a metal-metal and metal-carbon monoxide covalent bond. The carbonyl ligand is a strong  $\pi$ -acceptor that allows the metal to back donate into an empty  $\pi^*$  orbital which stabilizes low oxidation state systems (Figure 3).

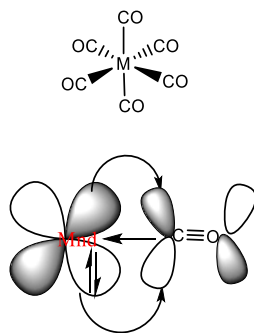


Figure 3: Transition metal carbonyl cluster

A typical carbonyl cluster has octahedral bonding; each metal back donates into the  $\pi^*$  orbital of the carbonyl ligand to form a covalent bond between metal and carbon.

A general reason to examine transition metal carbonyl clusters is to further our knowledge of organometallic catalysts. When organometallic complexes are added into reactions with a high activation energy, they catalyze the reaction by coordination of the substrate causing

a series of intermediate steps. This results in a lower activation energy, and an increase in the reaction rate. An example of how a metal complex may act as a catalyst is with the transition metal complex known as a Ziegler-Natta Polymerization of Alkenes (Figure 4). The  $\text{TiCl}_4$  is the organometallic catalyst that cause the polymerizing of alkenes and is commonly used for plastic synthesis.<sup>2</sup>

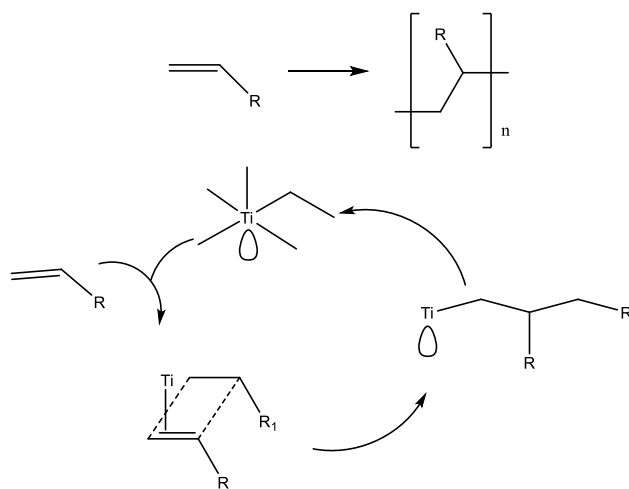


Figure 4: Sample Ziegler-Natta polymerizing different alkenes

It is imperative to know the mechanism of organometallic catalysis because knowing the process allows manipulation of the product direction. Reactions may proceed through multiple routes and produce multiple products, but if the mechanism is known it could be directed to form one product. In addition, an understanding of the mechanism and its multiple transition states may lead to understanding the thermodynamics and kinetics of the reaction. Typically, the second row transition metals form better organometallic catalysts (like ruthenium),<sup>3</sup> but multiple osmium carbonyl clusters have been reported to have catalytic properties.<sup>4</sup> An investigation of the bonding modes in these novel osmium complexes may lead to understanding the mechanisms of other catalysts with a similar structure and potentially improve the specificity of a catalyst.

## Bonding Transition Metal Complexes

Transition metal organometallic compounds contain a metal-organic ligand bond that follow the 18 electron rule. This rule states that all the electrons in the complex add up to 18 bonding electrons.<sup>3</sup> Additionally, this rule can predict the number of metal-metal covalent bonds and the structure of the transition metal complex. This rule applies to our starting material, Complex A, which predicts the two osmium-osmium bonds and the bridging structure of this compound, which was confirmed by X-ray crystallography (Figure 5).

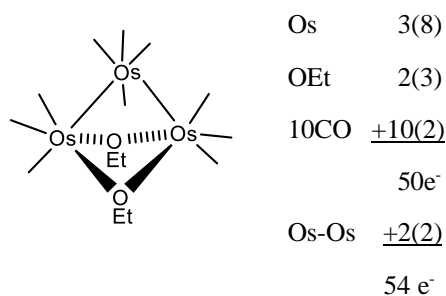


Figure 5: Electron Count of Complex A resulting in two Os-Os bonds.

This rule also applies to Isomers B, monomeric products  $\text{Os}_2(\text{CO})_6(\text{RCONH})_2$ , as seen in Figure 6.

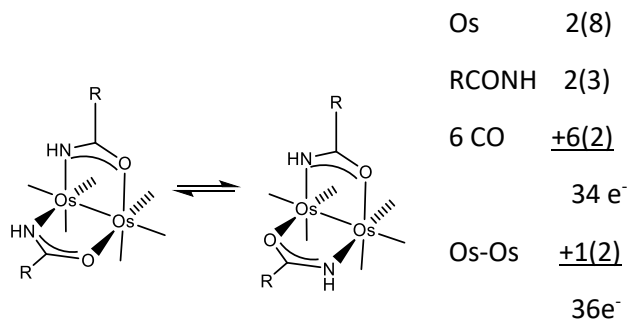


Figure 6: Electron Count of Complex B&C  $\text{Os}_2(\text{CO})_6(\text{RCONH})_2$  resulting in one Os-Os bond.

The results of the electron count predict that there are two electrons involved in an osmium-osmium bond. The complex researched in this paper is an organometallic carbonyl cluster which follows the 18 electron rule thus has the potential to be a catalyst.

## Amides as Ligands

Amides are ligands of interest because they can act in a bidentate fashion and serve as  $\pi$ -donor ligand at both metal-ligand bond sites (Figure 7).

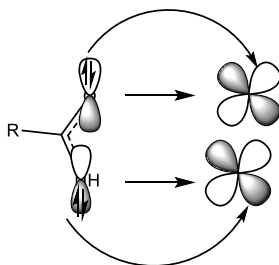


Figure 7: This is an amide acting as a bidentate  $\pi$ -donor

The presence of different donor atoms in amides leads to two possible conformational isomers, depending on the position of the donor atom. If there are two amides on a complex it will have two isomers; a head-to-head (H,H) isomer with both nitrogen atoms on the same end of the molecule, or a head-to-tail (H,T) isomer with nitrogen atoms on the complex (Figure 8).

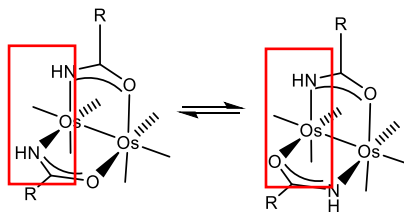


Figure 8: On the left is the (H,H) isomer and the right is the (H,T) isomer

Amide functional groups can be easily deprotonated, have nucleophilic activity, and have larger pH resistance range (buffer range).<sup>5</sup> On metal complexes this resistance causes amides to be a very tolerant catalysts, which is another reason to investigate amides.<sup>6</sup>

The reactivity of coordinated amides is of interest because amides are a biologically relevant functional group. In this research we work on is with primary amides, but future research could investigate the bonding and reactivity of secondary and tertiary amides.



Biologically amides are the foundation of every amino acid backbone and when polymerized (usually a dehydration reaction) are the base of proteins (Figure 9).<sup>7</sup>

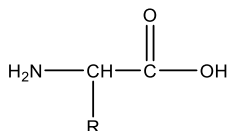


Figure 9: All amino acids have the same carbon back bone containing an amide group

Transition metals are known to participate in many biochemical reactions. The most commonly known protein with a transition metal is hemoglobin. Directly below the center of the four subunits in this structured protein is  $\text{Fe}^{2+}$  which is coordinated to  $\text{H}_2\text{O}$  and a histidine group and polyphyrin (Figure 10).<sup>7</sup> The Fe is oxidized to its 3+ state by a ligand exchange from  $\text{H}_2\text{O}$  to  $\text{O}_2$ . The  $\text{Fe}^{3+}$  state causes a planar structure, thus Fe is at the center of the heme group and the coordinate histidine is shifted up (Figure 10).<sup>2</sup> In simpler terms, the oxidation and reduction of  $\text{Fe}^{2+}$  causes the relaxed and tense states of hemoglobin and allows the transportation of  $\text{O}_2$ . Although this paper does not analyze hemoglobin, we do explore osmium which is in same group, thus will have similar reactivity.

#### *Anti-cancer Activity of Osmium Clusters and Analog species*

Transition metal complexes have long been known to have anti-cancer activity like cis-platin. Osmium carbonyl clusters have been investigated because some cells are becoming more resistant to cisplatin.<sup>8</sup> Osmium complexes have been studied for anticancer activity both in-vivo and in-vitro.<sup>9</sup> The osmium complexes are much larger than typically investigated transition metal complexes in this field and maintain three or more metal covalent bonds.<sup>10</sup> The findings in a recent article by Kong revealed five osmium clusters have anti-cancer activity:  $\text{Os}_3(\text{H})_2(\text{CO})_{10}$ ,  $\text{Os}_3(\text{CO})_{10}(\text{NCMe})_2$ ,  $\text{Os}_3(\text{H})(\text{OH})(\text{CO})_{10}$ ,  $\text{Os}_6(\text{CO})_{18}$ , and  $\text{Os}_6(\text{CO})_{10}(\text{NCMe})_2$  (Figure 11).<sup>10</sup>

These five complexes had significant anti-cancer activity against ovarian carcinoma. Kong proposed these clusters are active because of the bridging ligand and its ability to stimulate telomerase inhibition. The diamide complex in this paper has a similar structure to the clusters below and has potential to be an anti-cancer agent.

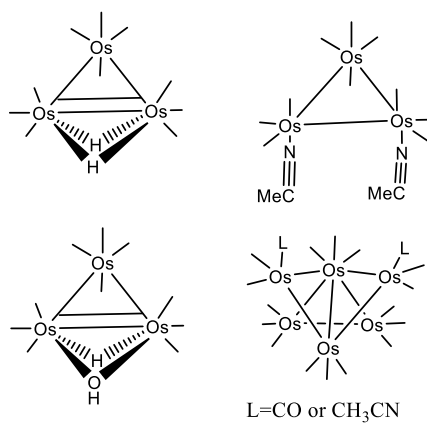
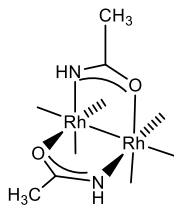


*Figure 11: Five carbonyl clusters tested for anti-cancer activity*

Additionally, osmium clusters may have some advantages compared to the platinum based cisplatin because it is larger and has the ability to bind to a wide variety of ligands.<sup>8</sup> Due to its large size it will have more coordination sites than found in cisplatin; thus it has the capacity to control the shape of the biological complex. Also osmium will experience different oxidation states than platinum and will undergo different bonding, which could access different anti-cancer mechanisms.

For example:

An analog structure to the complex investigated in this paper is a dirhodium diamide, head-to-tail complex, seen in Figure 12.<sup>11</sup> It is reported that the photo-product of the dirhodium diamide led to DNA covalent bonding at the Rh atom. This means the complex has the potential to modify or alter the DNA sequence.



All other bonds to Rh are  $\text{CH}_3\text{CN}$

Figure 12: Burya's research group found this structure to have the best anti-cancer activity.

### Research on Reactivity of Dibriged Di-and Triosmium Carbonyl Clusters

At Drew University, the Pearsall laboratory has been investigating novel triosmium structures with Complex A as a starting material. Complex A was first observed as a side product in the synthesis from  $\text{Os}_3(\text{CO})_{12}$  in 1984<sup>12</sup>, and with further investigation of its chemistry, it was revealed that it has different reactivity.<sup>13</sup> Complex A differs from the commonly used triosmiumdodecacarbonyl because it only has two metal-metal bonds. The Pearsall laboratory found that Complex A reacts to form other osmium complexes with alcohols or diols by substitution of the alkoxide ligand (Figure 13). These structures all have a bridging ligand similar to the osmium carbonyl clusters found to have anti-cancer activity.<sup>10</sup> Reactions of  $\text{Os}_3(\text{CO})_{10}(\text{OEt})_2$  with carboxylates,  $\text{Os}_2(\text{CO})_6(\text{RCOO})_2$ , and amides,  $\text{Os}_2(\text{CO})_6(\text{RCONH})_2$  led to formation of a diosmium complex as the more favorable species (Figure 14).

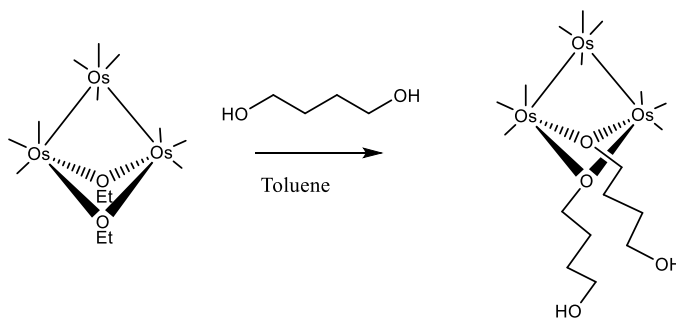


Figure 13: Maintain the triosmium structure with the reaction with a bridging ligand

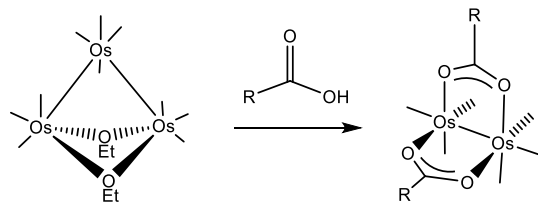


Figure 14: Osmium carbonyl cluster with a carboxylate synthesizing a dimer species

Diosmium carboxylate complexes,  $\text{Os}_2(\text{CO})_6(\text{RCOO})_2$ , were first discovered in 1969.

Triosmiumdodecacarbonyl was refluxed with a series of carboxylic acids at high temperature and pressures (Figure 15).<sup>14</sup> This was significant because an osmium atom was lost by an unknown mechanism. The more favorable structure is diosmium species not triosmium, due to the carboxylate acting as a bidentate ligand which is a better donor when trans to a  $\pi$ -acceptor. Also if the carboxylates were acting as trans ligands there would be too much steric strain and the carbonyl would not be  $180^\circ$ . The osmium atoms participate in the bonding and accepting of electron density from the  $\pi$  donor bonds.

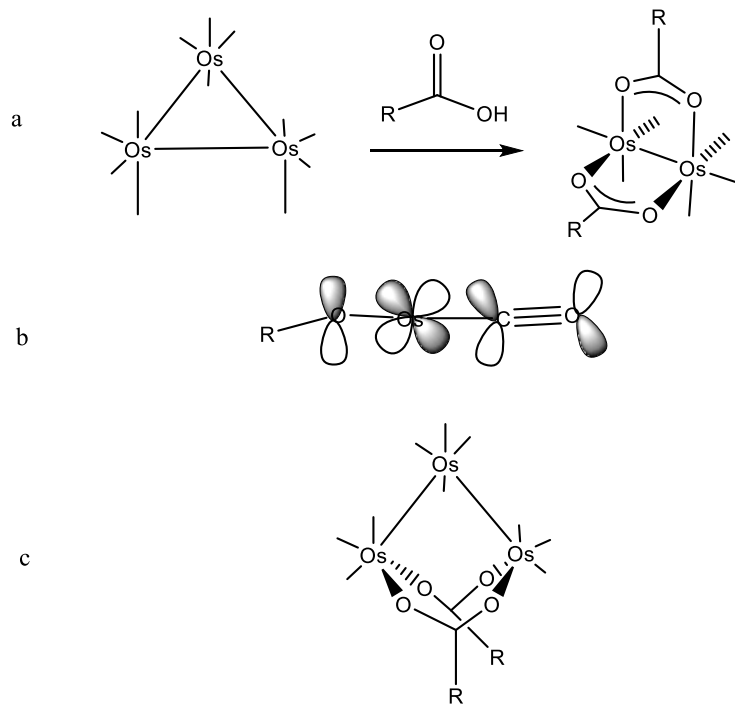
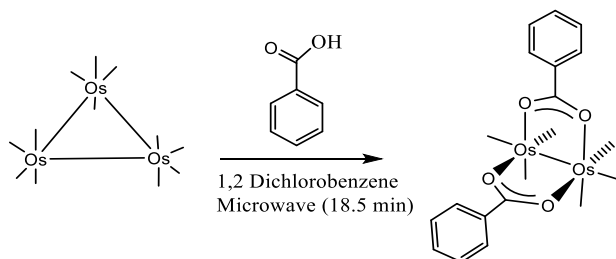


Figure 15: a) Earliest reported diosmium dimer. This was synthesized by carboxylic acid in acetic acid. R= Me b) The coordination of osmium to a  $\pi$ -donor and  $\pi$ -acceptor. c) The sterically hindered trans triosmium carbonylate structure

Subsequent research since 1969 has explored the complexes found using modern day technology, most recently by using microwave assisted reaction instead of traditional refluxing solvent.<sup>15</sup> The microwave assisted reactions led to a shorter reaction time, a larger yield, and a route into more substituents, such as a phenyl group (Figure 16). In addition, when using microwave technology under different conditions (shorter time) a triosmium structure was synthesized, obtained in a different reaction in 1998, but with other substituents<sup>16</sup>. A triosmium structure was also obtained, containing a bridging hydride and a PhCOO bidentate bridge.<sup>15</sup>



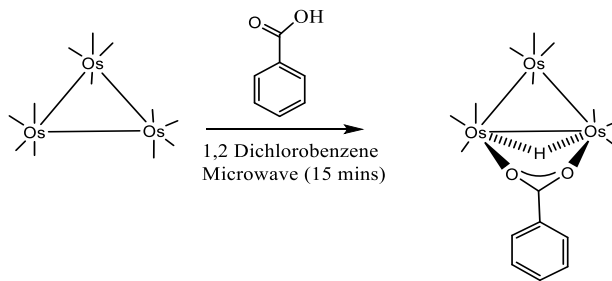


Figure 16: Two products that could be synthesized only with the aid of the microwaves technology. R= H, Me, Et, and Ph

Many researchers were interested in the triosmium species with the bidentate bridge as in Powell's work, because they hypothesized it was similar to the intermediate species leading to the diosmium carboxylate complex.<sup>15</sup> Ainscough and Brodie's group used the starting material, triosmiumdecacarbonylbisacetonitrile ( $\text{Os}_3(\text{CO})_{10}(\text{NCMe})_2$ ), because acetonitrile ligands are more labile.<sup>16</sup> They began using thiobenzoic acid instead of carboxylates to slow the reaction and isolate the triosmium bridged product,  $\text{Os}_3\text{H}_{10}(\text{C}_6\text{H}_4(\text{OH})(\text{COS}))$ , Figure 17. These findings shed a light onto the intermediate and the mechanism of the reaction.

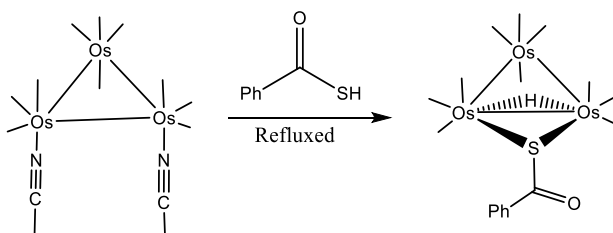


Figure 17: Triosmiumdecacarbonylbisacetonitrile and the intermediate triosmium species with one bidentate thiobenzoic acid.

The Pearsall research group found similar reactivity when using Complex A as a precursor.<sup>17,18</sup> When Complex A was heated with either acetic acid or propanoic acid in hexanes at a low temperature ( $60^\circ\text{C}$ ), they found an intermediate, Species A,<sup>17&18</sup> (Figure 18, 19) analogous to the one reported by Ainscough and Brodie, with carboxylate monodentate.<sup>16</sup> Furthermore, spectroscopic data showed the intermediate was in equilibrium with the second

isomer. For both acid they reported that the intermediate product reacted further to give the diosmium carboxylate product.

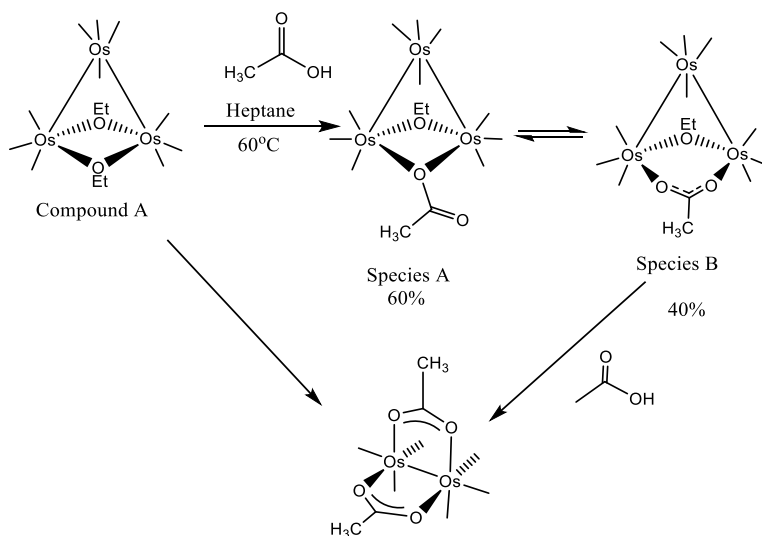


Figure 18: The reaction of acetic acid and Compound A with their equilibrium products.

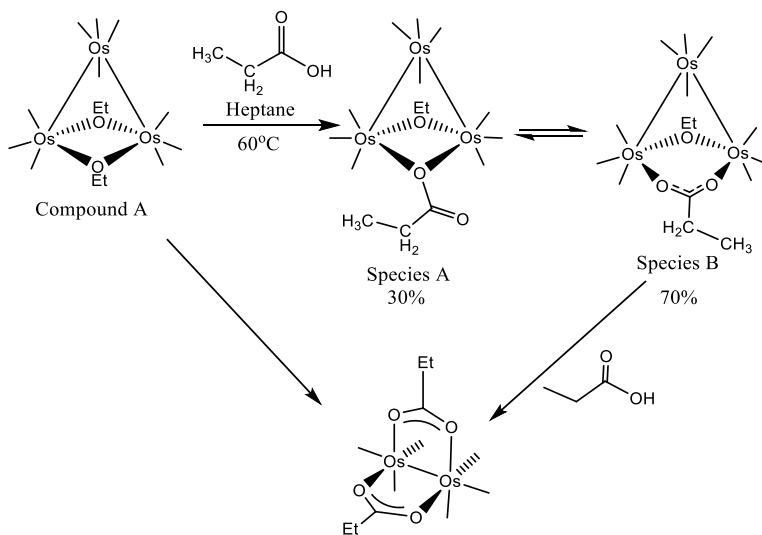


Figure 19: This was the reaction of propionic acid and Compound A with their equilibrium products.

The acetic acid reaction revealed a similar equilibrium ratio of 6:4 for the mono-substituted to bi-substituted products.<sup>18</sup> The equilibrium mixture for the propanoic acid was a ratio of 3:7. As the experiment continued, they proposed that the conversion to the diosmium complex occurred via

isomer B to another unstable intermediate before the loss of the non-bridged osmium atom (Figure 20).

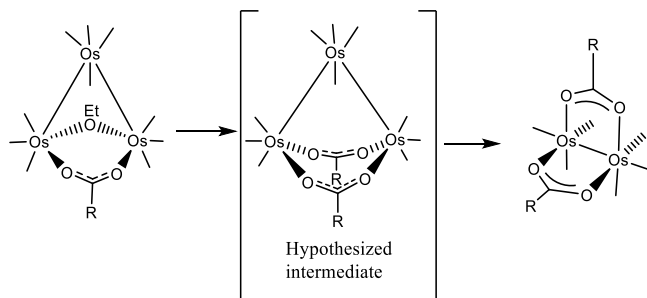


Figure 20: The center species is the hypothesized intermediate converted from isomer B.

Very little has been reported on the interactions of triosmium carbonyl clusters with amides. Odiaka has reported triosmium and diosmium amide products.<sup>19</sup> He investigated the triosmiumdecacarbonylbisacetonitrile,  $\text{Os}_2(\text{CO})_{10}(\text{MeCN})_2$ , with a series of amides. The major product was a triosmium species (Figure 21). A minor product, a diosmium diamide complex, was reported in 5% yield, but was left unexplored and no data was provided.

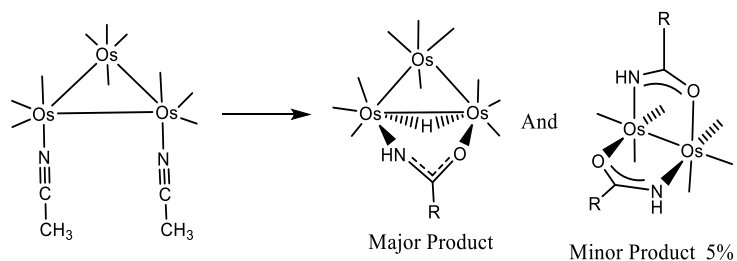


Figure 21: Triosmium with a bridging hydride and bidentate amide was the major product. One of many minor products was the head-to-tail isomer of the diosmium product. R= H, Me, Pr, Et, and Ph

## Polymers

Polymers are formed from monomeric units that bond together to form a large macromolecule. Polymers are commonly associated with proteins or plastics. Metal complexes



can also undergo polymerization leading to interesting chemical effects. For example, the known monomer,  $\text{Ru}_2(\text{CO})_6(\text{RCOO})_2$ , was polymerized by the displacement of the carbonyl ligands trans to the Ru-Ru, Figure 22.<sup>14</sup>

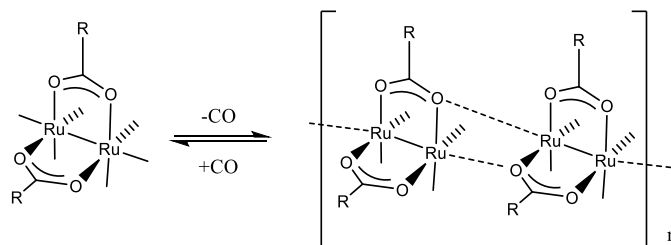


Figure 22: First mention of polymer with Carboxylate ligands in ruthenium complex

The products of reactions of the metal complex  $\text{Ru}_3(\text{CO})_{10}(\text{MeCN})_2$  with amides,  $\text{Ru}_2(\text{CO})_4(\mu_2, \eta^2\text{-HNOCPh})_2(\text{MeCN})_2$  and  $\text{Ru}_2(\text{CO})_4(\mu_2, \eta^2\text{-HNOCPh})_2(\text{PPh}_3)_2$ , have also been reported to polymerize. The polymers were composed of the monomeric units of cis-head-to-tail  $\text{Ru}_2(\text{CO})_6(\mu_2, \eta^2\text{-HNOCPh})_2$ <sup>20</sup> (Figure 23). It was proposed that a Ru oxygen bond connects the polymer units and that is easily displaced with the addition of excess ligand, resulting in the cis-head-to-tail structure.

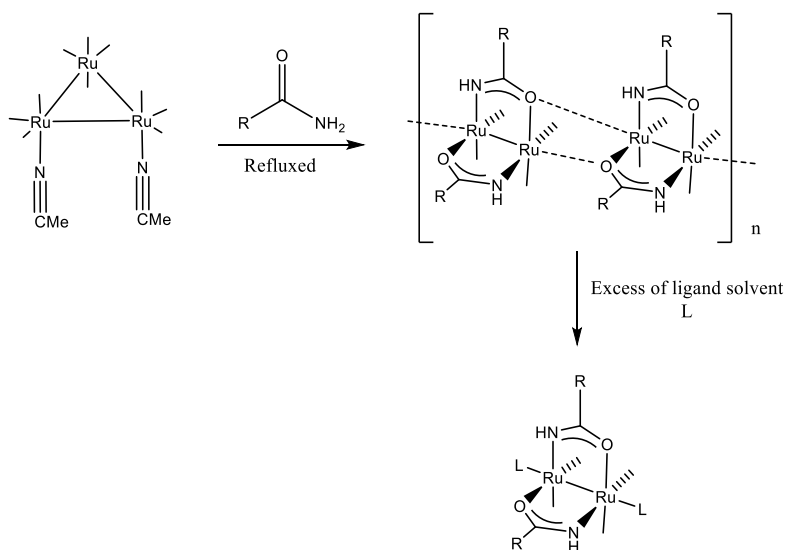


Figure 23: Diruthinium species and polymer with different amides HNOCPH and MeCN ligand. R= Me, Et, Pr, and Ph

### Previous research with the Pearsall Group

Recently the Pearsall group expanded their research previously done on carboxylates and began investigating the synthesis of the diosmium diamide complex as a major product.<sup>13</sup> Marak began with Complex A and analyzed its reaction with two different amides, acetamide and benzamide. This led to two diosmium diamide isomers found in equilibrium, Isomers B and C. Both amides, acetamide and benzamide, when reacted with Complex A led to two different isomer products, proposed to be the head-to-head and the head-to-tail isomers.<sup>13</sup> She reported the isomer ratios found at 110 °C for each amide. Isomers B had a head-to-tail to head-to-head ratio of 52:48. Isomers C had a head-to-tail to head-to-head ratio of 61:39. Marak found that it was only possible to isolate the head-to-head and head-to-tail of Isomers C. Nuclear magnetic resonance spectroscopy (NMR) revealed each isolated benzamide isomer would slowly reform to a mixture of both isomers, suggesting interconversion between the isomers.

This research expands on the work done by Marak, and further explores the interconversion reaction of the Isomers B over a range of temperatures.<sup>13</sup> In addition, it explores

the possible exchange of the coordinated amide on Isomer B with a free amide in solution (Figure 24).

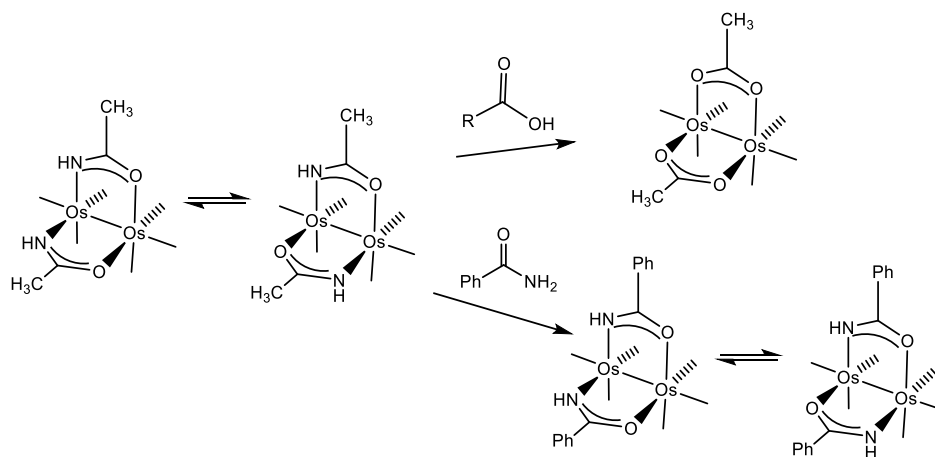


Figure 24: The investigation of the intramolecular exchange of the coordinated amide

During the synthesis of the monomers we also found a polymer product, which was investigated more in-depth (Figure 25).

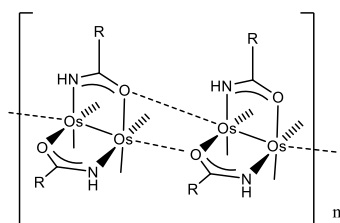


Figure 25: This is the proposed structure for the dioxmium amide polymer

Moreover, this research investigates microwave assisted synthesis of the dioxmium amide dimers, just as the Powell group did for the carboxylate monomer.<sup>15</sup> This research presents the first synthesis of the dioxmium amide complex that resulted in a good yield. This novel structure is interesting because it may have potential anti-cancer activity and the potential to inform design of new organometallic catalysts.

## Methods

### Infrared Spectroscopy

The more general use of infrared spectroscopy, or IR for short, involves excitation of a molecule with infrared light causing bond vibrations such as stretching and wagging which are characteristic of different functional groups on a molecule. While this technique can be useful for characterizing a molecule by identifying functional groups present or absent throughout a reaction, this work is primarily focused on IR in the carbonyl region ( $\sim 1600\text{-}2200\text{ cm}^{-1}$ ) to characterize our products. This technique is used for metal carbonyl compounds because the symmetry of the carbonyl ligands about the cluster will dictate the band patterns observed in the IR. Uncoordinated carbon monoxide (CO) ligands have a vibrational frequency of  $2143\text{ cm}^{-1}$ . When CO is coordinated to the metal, lower frequency vibrations are typically observed due to the back donation of the metal which reduces the energy of the CO bond vibration. Additionally, when more than one carbonyl ligand is coordinated to a metal they can vibrate in different modes with each other creating several vibrational bands dependant on the overall molecular symmetry. Looking at simple mono-nuclear compounds with more than one carbonyl ligand for example, one can see that a high symmetry compounds with ( $O_h$ ) symmetry like  $\text{Mo}(\text{CO})_6$  exhibit only one band as all the carbonyl ligands are in the same environment, while lower symmetry *cis*- $\text{Mo}(\text{CO})_4(\text{PH}_3)_2$  ( $C_{2v}$ ) exhibit several vibrational modes creating four distinct bands in its pattern (figure M.1).

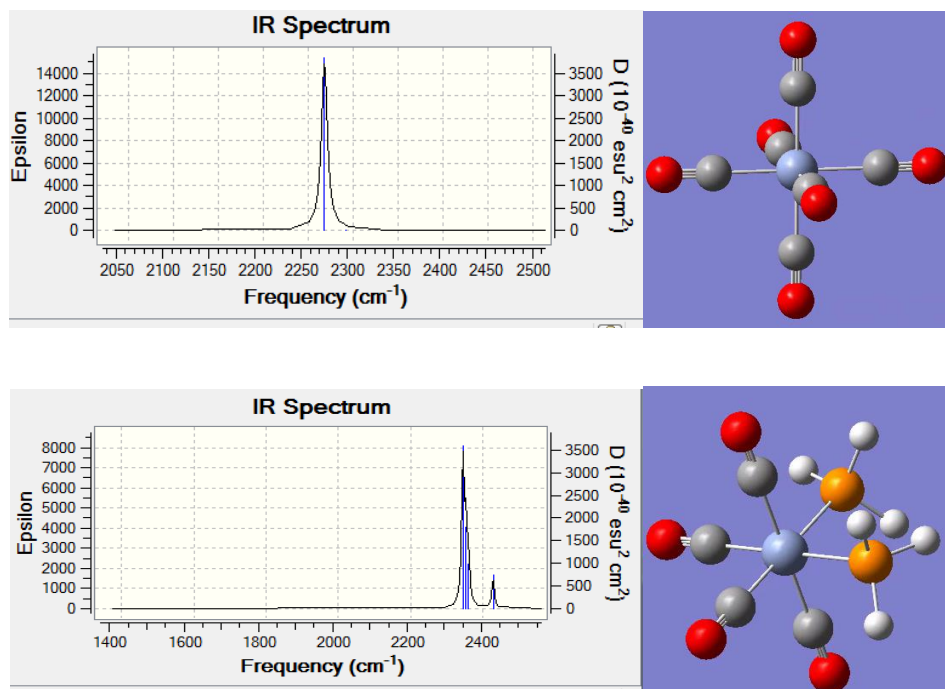


Figure M.1- Calculated vibrational band patterns of  $\text{Mo(CO)}_6$  (top) and  $\text{Mo(CO)}_4(\text{PH}_3)_2$  (bottom)

The effect of symmetry of the carbonyls on the band pattern. By extending this concept to higher nuclearity clusters it is possible to monitor a reaction and characterize products based on the symmetry of the carbonyl ligands. For example, an  $\text{Os}_3(\text{CO})_{10}(\mu^2\text{-X})_2$  cluster will have a band pattern as shown in figure 11, and this pattern will remain consistent for each X, where X could be OEt, OMe, Cl, Br, I, although the wavenumbers will shift depending on the strength of the ligand X. In comparison a compound used in this research, the  $\text{cis-Os}_2(\text{CO})_6(\mu^2\text{-X})_2$  cluster, has a higher level of symmetry than the above examples, so its observed band pattern is different than an  $\text{Os}_3(\text{CO})_{10}(\mu^2\text{-X})_2$  as seen in figure M.2.

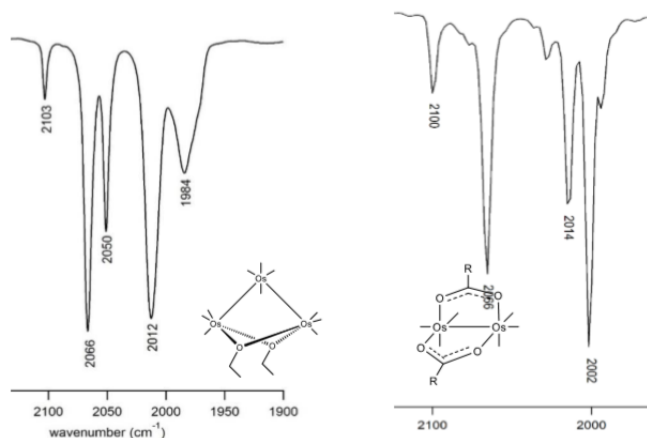


Figure M.2- Example of band patterns  $Os_3(CO)_{10}(\mu_2-X)_2$  class of cluster (left) and  $cis-Os_2(CO)_6(\mu_2-X)_2$  class of cluster (right) demonstrating the change in band pattern.

### Thin Layer Chromatography

Chromatography is a technique used to separate compounds based on intermolecular forces. In this work all osmium carbonyl clusters are separated using thin layer or preparative thin layer chromatography which separates compounds based on polarity. This technique utilizes a thin layer of silica coated on a plate which acts as the polar stationary phase. The plate is placed into a mixture of relatively nonpolar solvents making up the mobile phase. The compound or reaction mixture is spotted near the bottom of the plate so that it will lie just above the level of the mobile phase. Then, as the mobile phase travels up the vertical plate, the compounds will travel with it, with more polar compounds interacting more with the polar stationary phase and therefore remaining closer to the bottom of the plate than less polar compounds which travel more with the mobile phase. This setup can be seen in figure M.3.

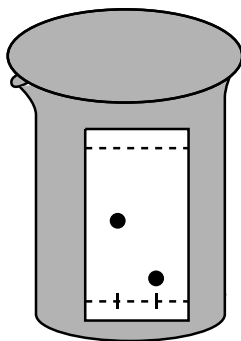


Figure M.3- TLC plate set up

The TLC plate can also give quantitative data designated the retardation factor, or  $R_f$  value, which describes the amount a compound moved up the plate compared to the amount the mobile phase moved (equation 1). This can be seen in figure M.4.

$$R_f = \frac{\text{Distance compound traveled}}{\text{Distance mobile phase traveled}} \quad (\text{Equation 1})$$

Compounds with higher  $R_f$  values are more non-polar than compounds with lower  $R_f$  values, and in the same mobile phase this can serve as a way to identify compounds of different polarities.

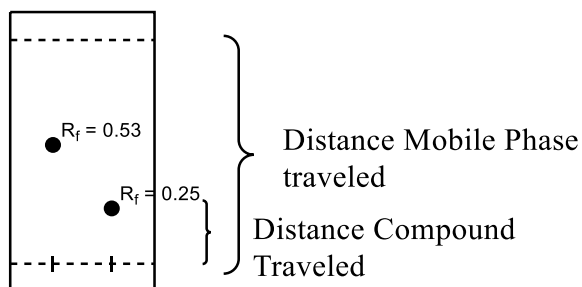


Figure M.4- Sample TLC plate with  $R_f$  parameters shown.

In general, this technique is used to monitor reactions to check for new product formation and consumption of starting material. This technique can also be employed on a larger scale, called preparative TLC, where the plate is considerably larger and made of glass, so at the end of

the chromatography compounds can be separated, scraped off and extracted from the silica. This was used in this investigation as a means of purification as well as separation of products.

### Nuclear Magnetic Resonance Spectroscopy

Nuclear magnetic resonance spectroscopy, or NMR, is a powerful tool in the characterization of compounds. This technique relies on the spin state of a magnet nucleus and location of this nuclear within the molecule relative to other atoms in a molecule. In the presence of a powerful magnetic field nuclear spins will align with this field. Then a perpendicular pulse of magnetic energy is applied and the received change on the magnetic coil gives insight to the structure of the molecule. For  $^1\text{H}$ -NMR, specifically the protons in a molecule are observed, and in the resulting spectrum, cluster of peaks represent a chemically unique proton which provides three types of information: chemical shift, integration, and multiplicity.

The chemical shift is dependent on the shielding or deshielding that a proton experiences in the presence or absence of electron withdrawing groups. For example, protons near to an electron withdrawing atom like oxygen, are considered deshielded and are shifted downfield, or to higher ppm. The opposite is true for electron donating groups which shield the proton and therefore lower the chemical shifts which appears more upfield.

Integration depends on the number of protons that are associated with a peak in the spectrum. For example, the methyl group ( $\text{CH}_3$ ) in n-propanol has three protons that are all in the same chemical environment so the peak associated with that group would have a relative integration of three, where the adjacent  $\text{CH}_2$  would have a relative integration of two. It is important to note that these integrations are relative to the other integrations in the spectrum, so symmetry in a molecule like butane would maintain a ratio of 3:2 even though there are 6 H that



are chemically equivalent for the two terminal methyls and 4 for the two CH<sub>2</sub> groups inside the chain. Integration can also be used to determine the ratios of more than one substance in an impure sample because the integrations are proportional to the amount of substance in a sample.

Multiplicity has to do with the “neighbors” of each chemically unique proton. This means the number of protons on each adjacent atom (with few exceptions) will interact with the proton in question and “split” the peak. In the propanol example the terminal methyl group has one adjacent carbon which has two protons bonded to it. These protons will split the single signal of the methyl protons into three. The splitting or multiplicity is 1+#of neighboring Hs, making protons with no neighbors a single peak called a singlet. On the other hand, one neighbor produces a doublet, two neighbors produces a triplet, three neighbors produces a quartet and so on. There also exists the possibility of two different neighbors which causes more complicated splitting. For example, in propanol one of the CH<sub>2</sub> has an adjacent methyl and another CH<sub>2</sub> which would create a triplet of quartets.

### Density Functional Theory Calculations

Electronic structure calculations can be used to gain insight into the energy of a system, optimize structures, and provide the theoretical vibrational spectrum which is what is most significant to this paper. In order to do this, density functional theory (DFT) calculations are used to approximate Schrödinger’s equation and find the ground state electronic energy which Hohenberg and Kohn, developers of DFT, demonstrated depends on the electron density of the system.<sup>21</sup> A commonly used hybrid functional was also employed, Becke 3-parameter Lee-Yang-Parr (B3LYP). The basis set used for these calculations also plays a significant role in the accuracy of the results. The Stuttgart group effective core potential (SDD) basis set was employed because it takes into account the high computational demand that would be required

for such a large atom like osmium and reduces the core electrons to an electrical potential rather than as approximate wave functions.<sup>22</sup> This reduces the number of basis set functions and therefore alleviates the computational demand for third row transition metal elements. This approximation is valid because the inner core electrons of third row transition metals are well shielded and therefore the chemistry is occurring at the frontier orbitals. SDD treats the valence electrons with a double zeta basis set, looking into the chemistry of 20 or fewer electrons on transition metal atoms which have total electrons ranging from 58-80 and approximates the core electrons as an electronic potential.<sup>22</sup> The vibrational frequencies are computed by taking the second derivatives of energy with respect to the nuclear coordinates of the structure with a subsequent transformation to mass-weighted coordinates. This is then converted to a readable theoretical IR spectrum.

This process treats the vibrations as harmonic rather than anharmonic, and this approximation can cause theoretical wave numbers to be higher in energy than experimental ones. In figure M.5, the harmonic approximation is a parabola where all energy transitions are equivalent. However, due to nuclear repulsions, the energy of a bond as a function of internuclear separation is a harmonic and is represented by the Morse potential. Here vibrational energy levels decrease with vibrational levels and there is a limit before the bond dissociates.

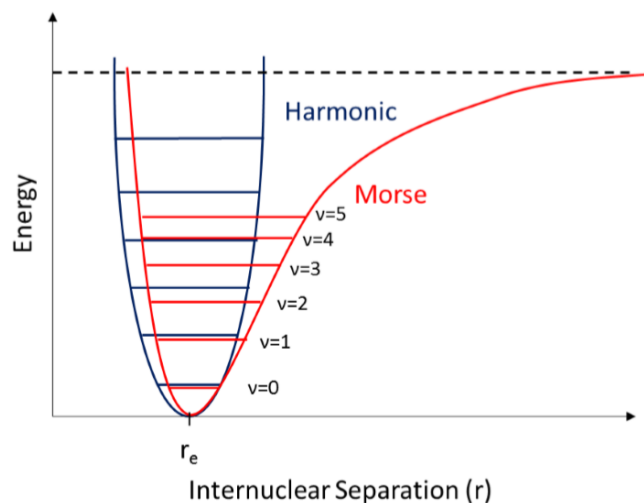


Figure M.5- The Harmonic Oscillator approximation as it relates to Morse potential

### Microwave Synthesis-

The microwave is a form of electromagnetic energy that uses frequency can impact the realm of molecular rotations. The electric field of a microwave heats matter by dielectric heating. As the electric field passes through a sample, energy is transferred to molecules through the mechanisms of dipole rotation and ionic conduction. Because microwave heating is so efficient, temperatures up to 300 °C in a matter of minutes. Overall the microwave is a safe flexible and easily reproduces reactions.<sup>23</sup>

## Experimental

### *Synthesis of $Os_2(CO)_6(RCONH)_2$ using $Os_3(CO)_{10}(OEt)_2$ and acetamide in toluene at 110° C*

$Os_3(CO)_{10}(OEt)_2$  (20 mg, 0.0204 mmol) and acetamide (15 mg, 0.254 mmol) were stirred in toluene (10 mL) at 110 °C for 2 hours. Overall, the experiment started as a light yellow solution and changed to a light brown. A TLC with a 40% ethyl acetate/ 60% hexanes solvent system revealed the product, amide dimers, and the starting material  $Os_3(CO)_{10}(OEt)_2$ . The TLC of the mixture shows a baseline product and two spots. The major product had an  $R_f = 0.19$  (more polar) and the second product at  $R_f = 0.85$ . The IR confirmed the product of  $Os_2(CO)_6(CH_3CONH)_2$  (vCO, toluene) with peaks at 2086.8  $cm^{-1}(m)$ , 2048.9  $cm^{-1}(s)$ , 1991.9  $cm^{-1}(m)$ , 1972.1  $cm^{-1}(m)$ , 1709.6  $cm^{-1}(w)$ , and 1688.6  $cm^{-1}(w)$ .

### *Synthesis of $Os_2(CO)_6(RCONH)_2$ using $Os_3(CO)_{10}(OEt)_2$ and benzamide in toluene at 110° C*

$Os_3(CO)_{10}(OEt)_2$  (23 mg, 0.0235 mmoles) and benzamide (59 mg 0.480 mmoles) in were mixed toluene (10 mL) and brought to reflux at 110°C under nitrogen for 75 minutes. The experiment started as a light yellow solution and became a light brown solution. TLC 20% ethyl acetate / 80% hexanes solvent system monitored the reaction and there were three spots. The major product was at  $R_f=0.22$  the second product  $R_f= 0.34$  and the last at  $R_f= 0.85$ . The IR confirmed  $Os_2(CO)_6(PhCONH)_2$  isomers were the major products (vCO, toluene) with peaks at 2087.6  $cm^{-1}(m)$ , 2076.8  $cm^{-1}(w)$ , 2050.9  $cm^{-1}(s)$ , 2025.7  $cm^{-1}(w)$ , 1996.8  $cm^{-1}(m)$ , 1978.3  $cm^{-1}(w)$ , and 1689.8  $cm^{-1}(m)$ .

### *Exchange of the coordinated amide on $Os_2(CO)_6(RCONH)_2$ with free carboxylic acid*

$Os_2(CO)_6(CH_3CONH)_2$  (10 mg 0.00885 mmoles) and glacial acetic acid (0.1 ml 0.00167mmoles) was refluxed in toluene at 110°C under nitrogen for 120 min. Overall, no observable change was seen. The reaction was monitored by TLC with a 40% ethyl acetate/ 60%

hexanes solvent one band (0.19) and a baseline product form. The IR band pattern ( $\nu_{\text{CO}}$ ) of 2086.8  $\text{cm}^{-1}$ (w), 2070.1  $\text{cm}^{-1}$ (s), 2050.2  $\text{cm}^{-1}$ (s), 1991.9  $\text{cm}^{-1}$ (m), 1972.1  $\text{cm}^{-1}$ (m), 1709.6  $\text{cm}^{-1}$ (s), and 1688.6  $\text{cm}^{-1}$ (w), confirmed no new product was formed.

*Synthesis of the Acetamide-Polymer  $[\text{Os}_2(\text{CO})_4(\text{CH}_3\text{CONH})_2]_n$  in toluene at 110° C*

$\text{Os}_3(\text{CO})_{10}(\text{OEt})_2$  (20 mg, 0.0204 mmol) and acetamide (15 mg, 0.254 mmol) were stirred in toluene (10 mL) at 110 °C for 4 hours to provide unreacted Compound A and the polymer. Overall, the observable changes in the experiment were a color change from a light yellow solution to a gray-brown with a semi soluble precipitate. The reaction was monitored by TLC and IR. The TLC used 40% ethyl acetate/ 60% hexanes solvent system. The  $R_f$  value for Compound A is 0.85 and the  $R_f$  value for the polymer, Compound D, was 0. The IR, at a range of 2200  $\text{cm}^{-1}$  to 1500  $\text{cm}^{-1}$ , was used to confirm the presence of the polymer,  $\text{Os}_2(\text{CO})_4(\text{CH}_3\text{CONH})_2$ . The reaction mixture had peaks at ( $\nu_{\text{CO}}$ , toluene) 2086.8  $\text{cm}^{-1}$ (m), 2070.1  $\text{cm}^{-1}$ (w), 2048.9  $\text{cm}^{-1}$ (s), 1991.9  $\text{cm}^{-1}$ (m), 1972.1  $\text{cm}^{-1}$ (m), 1709.6  $\text{cm}^{-1}$ (w), and 1688.6  $\text{cm}^{-1}$ (w).

*Reversal of the Acetamide-Polymer  $[\text{Os}_2(\text{CO})_4(\text{CH}_3\text{CONH})_2]_n$  in toluene at 110° C with CO (g)*

Compound D was refluxed at 110° C while bubbling CO(g) for 30 minutes. The product was the monomer complex. The observable changes to the solution was a gray-brown with a semi soluble precipitate to a light brown solution. This was confirmed with IR ( $\nu_{\text{CO}}$ , toluene) 2086.8  $\text{cm}^{-1}$ (m), 2048.9  $\text{cm}^{-1}$ (s), 1991.9  $\text{cm}^{-1}$ (m), and 1972.1  $\text{cm}^{-1}$ (m). The 40% ethyl acetate/ 60% hexanes solvent system TLC had only two bands, the monomer complex ( $R_f = 0.19$ ) and the Compound A ( $R_f = 0.85$ ), and no baseline product present.

*$\text{Os}_3(\text{CO})_{10}(\text{OEt})_2$  with Acetic Acid in Cyclohexane at 80° C*

$\text{Os}_3(\text{CO})_{10}(\text{OEt})_2$  (5 mg, 0.0051 mmol) and a drop of glacial acetic acid was stirred in cyclohexanes (5 mL) at 60 °C for 30 minutes a white precipitate was obtained. The TLC in 20% dichloromethane/ 80% hexanes solvent system revealed only a band for Compound A. In the IR the scan before the reaction started was 2104.2  $\text{cm}^{-1}$ , 2051.4  $\text{cm}^{-1}$ , 2066.8  $\text{cm}^{-1}$ , 2012.3  $\text{cm}^{-1}$ , 1988.7  $\text{cm}^{-1}$ , and 1598.9  $\text{cm}^{-1}$ . At the end the spectrum peaks were 2104.2  $\text{cm}^{-1}$ , 2051.4  $\text{cm}^{-1}$ , 2066.8  $\text{cm}^{-1}$ , 2012.3  $\text{cm}^{-1}$ , and 1988.7  $\text{cm}^{-1}$ .

*Synthesis of the Acetic Acid-Polymer  $\text{Os}_2(\text{CO})_4(\text{OOCCH}_3)_2$  in toluene at 110° C and Reversal with CO (g)*

$\text{Os}_2(\text{CO})_6(\text{OOCCH}_3)_2$  (5 mg, 0.0758 mmol) and a drop of glacial acetic acid was stirred in toluene (10 mL) at 110 °C for 30 minutes. The TLC used 20% dichloromethane/ 80% hexanes solvent system. The  $R_f$  value for the polymer was at the baseline. The IR confirmed the product of  $\text{Os}_2(\text{CO})_4(\text{OOCCH}_3)_2$  ( $\nu\text{CO}$ , toluene) in reaction mixture with peaks at 2091.7  $\text{cm}^{-1}(\text{w})$ , 2065.6  $\text{cm}^{-1}(\text{s})$ , 2000.7  $\text{cm}^{-1}(\text{w})$ , and 1921.1  $\text{cm}^{-1}(\text{s})$ . Over time the IR confirms the presence of the monomer ( $\nu\text{CO}$ , toluene) 2099.7  $\text{cm}^{-1}(\text{m})$ , 2065.6  $\text{cm}^{-1}(\text{m})$ , 2000.7  $\text{cm}^{-1}(\text{w})$ , and 1921.1  $\text{cm}^{-1}(\text{s})$ . When the polymer had CO (g) bubbled directly the IR confirmed the immediate decomposition of the polymer into the monomer species ( $\nu\text{CO}$ , toluene) 2099.7  $\text{cm}^{-1}(\text{s})$ , 2065.6  $\text{cm}^{-1}(\text{w})$ , 2014.1  $\text{cm}^{-1}(\text{m})$ , and 1998.6  $\text{cm}^{-1}(\text{w})$ .

*Microwave reaction of  $\text{Os}_3(\text{CO})_{12}$  and benzamide*

$\text{Os}_3(\text{CO})_{12}$  (20mg, 0.022 mmoles) and benzamide (51 mg, 0.417mmols) were mixed in cyclohexane (14 mL) and microwaved for 10 minutes at 150°C and 300W. The observable change was color change from a yellow solution to a brown solution. A TLC, with a 2/8 mixture of ethyl acetate and hexanes, showed 6 products with  $R_f$  values of; 0.10, 0.22, 0.34, 0.38, 0.59,

and 0.66. A silica column using a 40% ethyl acetate/ 60% hexanes solvent system was implemented. The 5 products were eluted in ethyl acetate and could be distinguished by color; the major product was a visible yellow, clear band, two other bands both light brown, and a yellow. The yellow was  $\text{Os}_3(\text{CO})_{12}$  and the clear bands were excess benzamide. The major product shown ( $\nu\text{CO}$ ,  $\text{CH}_2\text{Cl}_2$ ) 2077.5  $\text{cm}^{-1}$ , 2067.9  $\text{cm}^{-1}$ , and 2025.9  $\text{cm}^{-1}$ . An  $^1\text{H}$ NMR was obtained to analyze the structure further containing two peaks -13 and -20 ppm . The other two products were the different isomers of the benzamide dimer. The IR pattern is ( $\nu\text{CO}$ ,  $\text{CH}_2\text{Cl}_2$ ) 2087.6  $\text{cm}^{-1}$ , 2050.9  $\text{cm}^{-1}$ , 1978.3  $\text{cm}^{-1}$ , and 1689.8  $\text{cm}^{-1}$ .

*Microwave reaction of  $\text{Os}_3(\text{CO})_{10}(\text{OEt})_2$  with benzamide*

$\text{Os}_3(\text{CO})_{10}(\text{OEt})_2$  (20 mg, 0.0204 mmols) and benzamide (51 mg, 0.417mmols) were in cyclohexane solution and microwaved for 10 minutes at 150°C and 300W. The major product was the benzamide dimer, in a mixture containing starting material. The TLC, with a mixture of 6/4 ethyl acetate and hexanes, confirmed this with two bands with an  $R_f$  of 0.18, Compound 1, and the major product at 0.59, a mixture of Isomers C. This was determined by IR ( $\nu\text{CO}$ , dichloromethane) 2104.5  $\text{cm}^{-1}$ , 2067.9  $\text{cm}^{-1}$ , 2087.6  $\text{cm}^{-1}$ , 2050.9  $\text{cm}^{-1}$ , 1978.3  $\text{cm}^{-1}$ , and 1689.8  $\text{cm}^{-1}$ . Observable change was a yellow solution to a light brown solution. No further, experimentation was done with this product.

*The experimental synthesis of  $\text{Os}_2(\text{CO})_6(\text{OEt})(\text{COOCH}_3)$  with  $\text{CO}(g)$*

$\text{Os}_3(\text{CO})_{10}(\text{OEt})_2$  (10 mg, 0.0102 mmols) and a drop of acetic acid in toluene solution and refluxed with  $\text{CO}(g)$  bubbling through the reaction for 45 mins. The initial IR of the reaction mixture had Compound A and carboxylic acid and 45 mins later the IR of the reaction mixture contained no carboxylic acid. The TLC, with a mixture of 2/8 ethyl acetate and

dichloromethane, confirmed this with one band Rf of 0.85, Compound A. This was determined by IR ( $\nu_{\text{CO}}$ , dichloromethane)  $2104.5\text{ cm}^{-1}$ ,  $2067.9\text{ cm}^{-1}$ ,  $2050.9\text{ cm}^{-1}$ ,  $2012.6\text{ cm}^{-1}$ , and  $1988.3\text{ cm}^{-1}$ . Observable change was a light yellow solution to a light yellow solution with a white solid. No further, experimentation was done with this product.



## Results and Discussion

### *Synthesis of $Os_2(CO)_6(RCONH)_2$ and $Os_2(CO)_4(RCONH)_2$*

As mentioned previously in the introduction and methods; IR, TLC, and  $^1H$  NMR were used to monitor and analyze the reactions. Figure R.1 shows the unique stretching vibrations of the carbonyl ligands of starting material, Compound A. Its signature band pattern is a small weak peak, two thin intense peaks (the second shorter than the first), and two wide and intense peaks (the second shorter than the first) indicating the specific symmetry of Compound A's ten carbonyl ligands.

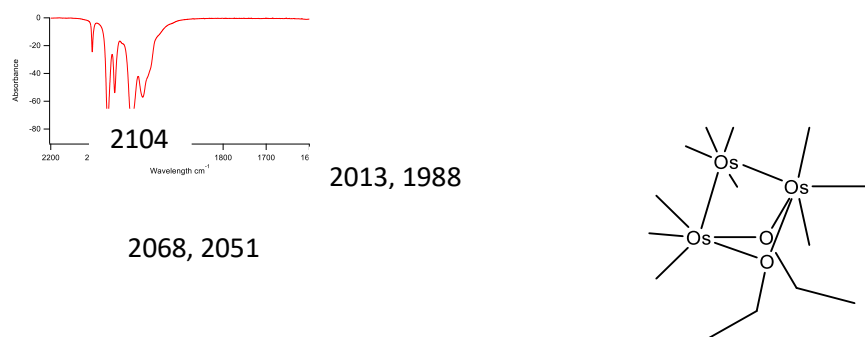


Figure R.1: IR of Triosmiumdecarbonylbisethoxide

Pure bisethoxide crystals dissolved in dichloromethane ( $CH_2Cl_2$ ). The IR peaks are: 2104  $cm^{-1}$ , 2068  $cm^{-1}$ , 2051  $cm^{-1}$ , 2013  $cm^{-1}$ , and 1988  $cm^{-1}$ .

### Reaction of A with Acetamide to give $Os_2(CO)_6(CH_3CONH)_2$

Compound A when refluxed with acetamide for 120 mins produced a mixture of Isomers B and unreacted Compound A, Figure R.3. In comparison to the pure bisethoxide IR (Figure R.1), the pure diosmium diacetamide, Isomers B, spectrum has only four important peaks lying at lower in wavenumber (Figure R.2). The typical band pattern that identifies Isomers B is sharp and intense, short and weak, sharp and intense, and wide and intense corresponding to the specific symmetry of the 4 carbonyls of Isomers B.

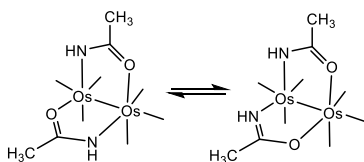
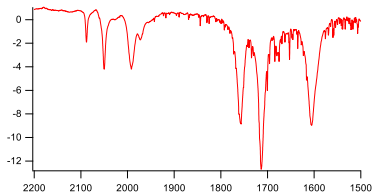
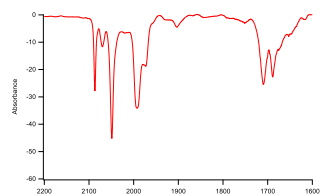


Figure R.2: Pure Isomer in  $\text{CH}_2\text{Cl}_2$

This is purified acetamide monomer containing both isomers and its IR spectrum was taken in  $\text{CH}_2\text{Cl}_2$ :  $2088\text{ cm}^{-1}$ ,  $2050\text{ cm}^{-1}$ ,  $1992\text{ cm}^{-1}$ , and  $1972\text{ cm}^{-1}$ .



a

b

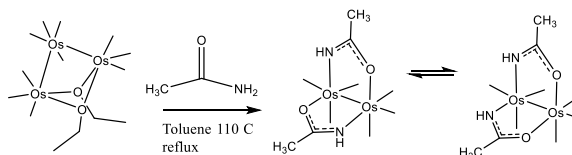


Figure R.3: Reaction mixture of the B Isomers

This is the Compound A reaction mixture with acetamide after 120 mins of reflux. The IR spectrum was taken in  $\text{CH}_2\text{Cl}_2$ :  $2088\text{ cm}^{-1}$ ,  $2050\text{ cm}^{-1}$ ,  $1992\text{ cm}^{-1}$ , and  $1972\text{ cm}^{-1}$ . Peak "a"  $2075\text{ cm}^{-1}$  is the polymer of acetamide. The peaks labeled "b" at  $1705\text{ cm}^{-1}$  and  $1678\text{ cm}^{-1}$  are acetamide in solution.

However, before the reaction was purified the IR had an unknown small peak at  $2075\text{ cm}^{-1}$ , as seen in Figure R.3. This peak was proposed to be the polymer, Compound D, but was not isolated. TLC was done for the mixture and confirmed the formation of a more polar product, the B Isomers  $R_f=0.19$  (Figure R.4). The TLC also contained a baseline product that could not be extracted from the TLC, and it is assumed to be Compound D.

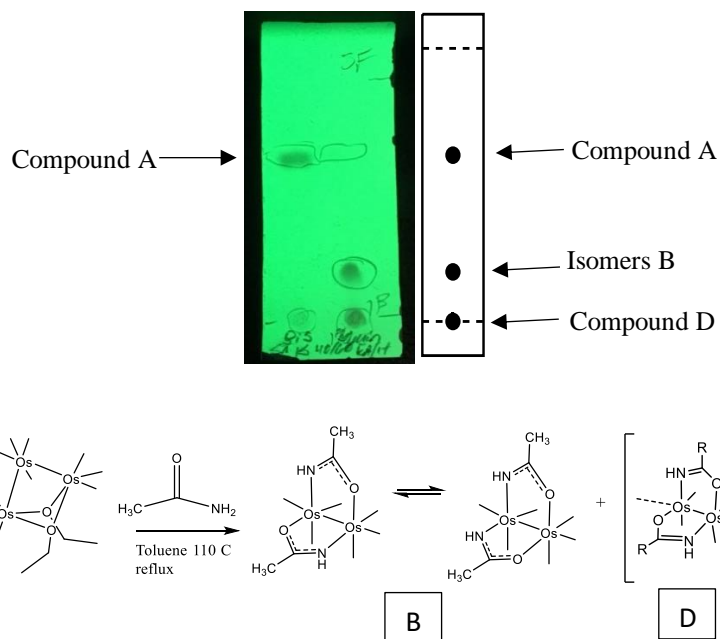


Figure R.4: the TLC of the reaction mixture of B Isomers.

### Formation of Polymer $[\text{Os}_2(\text{CO})_4(\text{CH}_3\text{CONH})_2]_n$ Compound D

In attempts to isolate the baseline product, Compound D, the solution was refluxed in toluene until the  $2075\text{ cm}^{-1}$  peak became more intense while the major Isomers B peak,  $2088\text{ cm}^{-1}$ , weakened in the background (Figure R.5). Additionally, this reaction was monitored by TLC, showing that as the  $2088\text{ cm}^{-1}$  weakened the Isomers B spot faded. The reaction mixture began as a light yellow/brown solution and became a gray-brown color with a cream like texture. Based on IR it was proposed that this product was a polymer Compound D, similar to the Ru analog mentioned in the introduction<sup>20</sup> (Figure R.6).

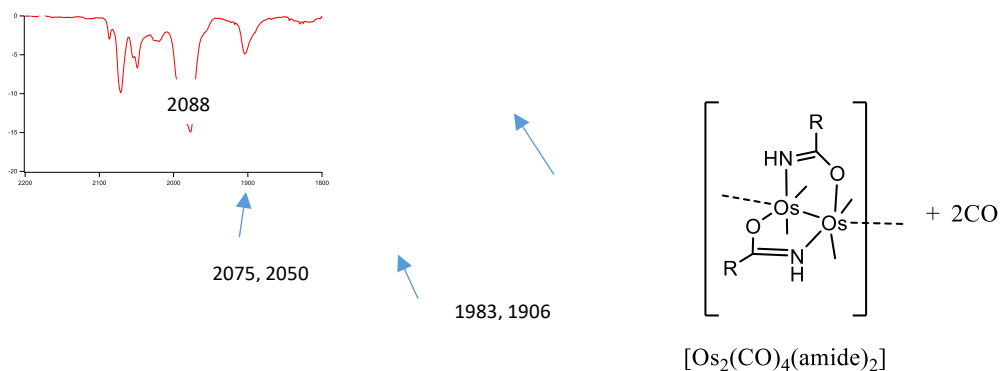


Figure R.5: Compound D in reaction mixture

Peaks for the semi-soluble polymer. The IR spectrum was taken in  $\text{CH}_2\text{Cl}_2$ : The peaks indicated with arrows are the Compound D peaks, at  $2075\text{ cm}^{-1}$ ,  $1983\text{ cm}^{-1}$ , and  $1906\text{ cm}^{-1}$ . The others are from the isomers B at  $2088\text{ cm}^{-1}$ ,  $2050\text{ cm}^{-1}$ , and  $1992\text{ cm}^{-1}$ .

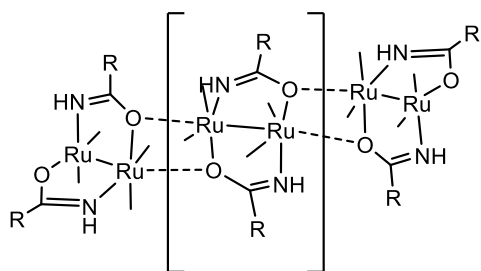


Figure R.6: Suss-Fink ruthenium polymer

As the Suss-Fink lab was able to break the the Ru-O bond for a different ligand.<sup>20</sup> I then experimented with trying to break the Os-O bond and revert the polymer, Compound D, back to the monomer, Isomers B. In the presence of excess carbon monoxide gas in refluxing in toluene, the polymer reverts back to the monomer. Thus I propose this reaction sequence, Figure R.7:

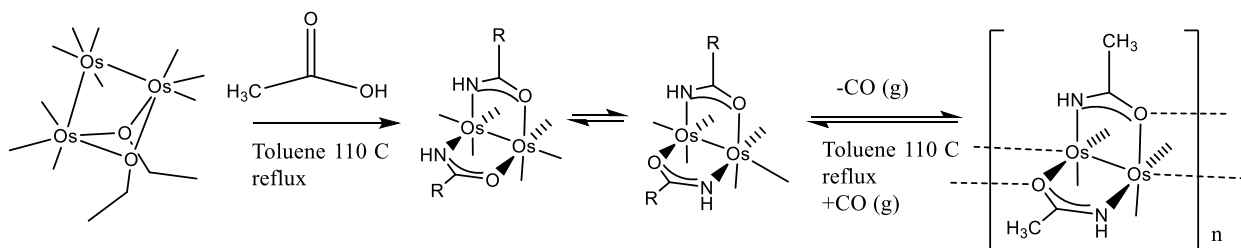


Figure 7: The proposed reaction scheme of Compound A to Compound D. Unknown if polymer is a H,H or H,T mixture or mixture of both isomers.

### Effect of Heat on $\text{Os}_2(\text{CO})_6(\text{CH}_3\text{COO})_2$

As mentioned in the introduction, a polymer of the diosmium carboxylate was seen under extreme conditions in 1964 by Crooks<sup>14</sup>, but left with no further analysis. I experimented trying to obtain the carboxylate polymer by refluxing the diosmium diacetate in toluene. The effect of heat on the known diosmium diacetate  $[\text{Os}_2(\text{CO})_6(\text{CH}_3\text{COO})_2]$  was investigated and found to also form a polymer, as seen in Figure R.8.

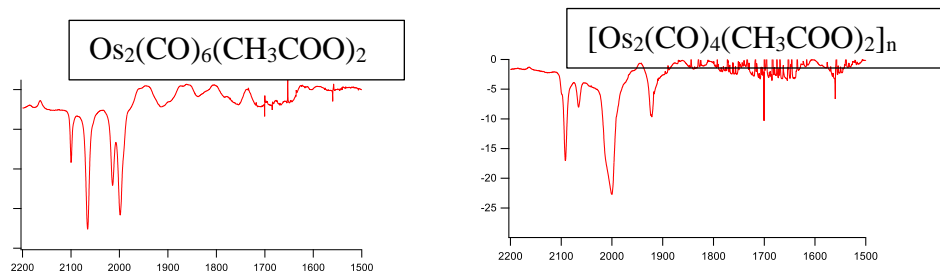


Figure R.8: Monomer and polymer IR for the diosmium carboxylate

The peaks for the monomer are  $2100\text{ cm}^{-1}$ ,  $2066\text{ cm}^{-1}$ ,  $2014\text{ cm}^{-1}$ ,  $2002\text{ cm}^{-1}$  which change to resemble the stretching patterns of only 4 carbonyl groups at  $2091\text{ cm}^{-1}$ ,  $2000\text{ cm}^{-1}$ ,  $2066\text{ cm}^{-1}$ , and  $1894\text{ cm}^{-1}$

If left with no addition of carbon monoxide the polymer will readily decompose to the monomer species, suggesting that the monomer is the more stable conformation. The proposed acetamide polymer, Compound D  $[\text{Os}_2(\text{CO})_4(\text{CH}_3\text{CONH})_2]_n$ , is more stable than the carboxylate polymer and requires addition of carbon monoxide to revert to the monomer. The  $[\text{Os}_2(\text{CO})_4(\text{CH}_3\text{COO})_2]_n$  polymer is less stable than the  $[\text{Os}_2(\text{CO})_4(\text{CH}_3\text{CONH})_2]_n$  polymer. Additionally, no polymer product were observed with  $[\text{Os}_2(\text{CO})_4(\text{PhCONH})_2]_n$  polymer. This suggests the relative stabilities:

Table 1. Stabilization of the polymer

$\text{Os}_2(\text{CO})_4(\text{PhCONH})_2]_n$	$[\text{Os}_2(\text{CO})_4(\text{CH}_3\text{COO})_2]_n$	$[\text{Os}_2(\text{CO})_4(\text{CH}_3\text{CONH})_2]_n$
<b>No polymer forms</b>	Polymer reverts to the monomer at room temperature	Polymer reverts to monomer at 110 °C

The reasons for the difference in the stability of the polymers is unknown. I theorize that it is due to the conjugated system and the amount of electron density withdrawn from the phenol group does not allow a stable Os-O bond. Also for the carboxylate polymer containing 2 oxygens disperses the electron density, thus not allowing for a stable Os-O bond.

### Reaction of Compound D with Acetonitrile

Compound D was dissolved in the labile ligand, acetonitrile, leading to a new product proposed to be  $[\text{Os}_2(\text{CO})_4(\text{NCCH}_3)_2(\text{CH}_3\text{COO})_2]$ , Figure R.9. Based on the results of the Suss-Fink paper,<sup>20</sup> I propose the osmium oxygen bonds are replaced with acetonitrile ligands because of how easily the polymer species decomposes to the monomer.<sup>20</sup> The theoretical infra-red spectrum of the proposed structure was calculated using Gaussian. Data were calculated following optimization using ground state DFT-B3LYP and basis set SDD in default solvation for heptane. The results indicated a simple 2 band spectrum (Figure R.10). This spectrum is shifted to a higher frequency because it is not following accounting for the solvent effect, so the two bands will be around  $2200 \text{ cm}^{-1}$  not the theoretical  $2500 \text{ cm}^{-1}$ .

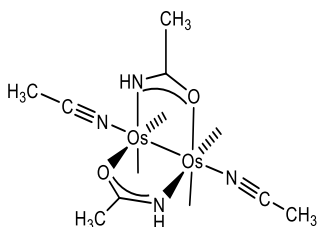


Figure R.9: Proposed structure of Compound D reaction with acetonitrile

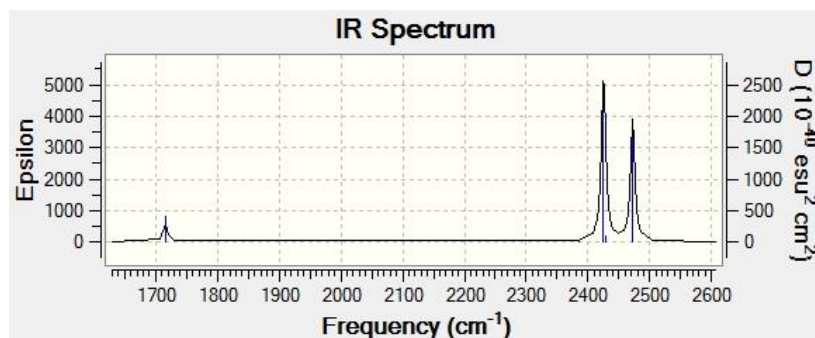


Figure R.10: Theoretical spectrum of  $Os_2(CO)_4(NCCH_3)_2(CH_3CONH)_2$

The theoretical spectrum closely resembles the experimental IR, having the two characteristic bands and the first being less intense than the second (Figure R.11) A TLC of the product was taken confirming a mix of products due to the multiple spots on the TLC which possibly correspond the two isomers, H,T and H,H, of  $Os_2(CO)_4(NCCH_3)_2(CH_3CONH)_2$  (Figure R.11). This is only preliminary data and merits further investigation.

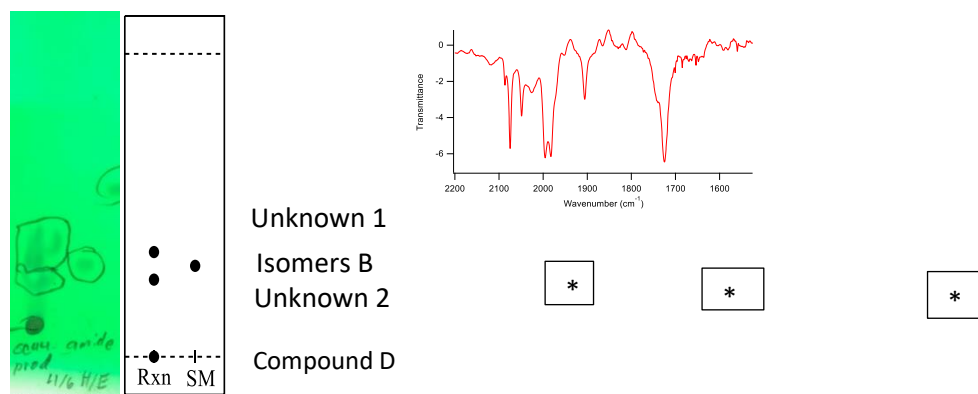


Figure R.10: IR of Compound D dissolved in acetonitrile and TLC comparing this product vs the Compound D vs Compound A

### The Thermodynamic Analysis of $Os_2(CO)_6(CH_3CONH)_2$ using $^1H$ -NMR-

Due to inability to separate the  $Os_2(CO)_6(CH_3CONH)_2$  isomers, we continued to explore the interconversion of the head-to-tail to head-to-head of Isomers B. Using  $^1H$ -NMR (Figure R.12). The peaks due to each of the isomers were assigned based on Marak's assessments of the electronegative effect on the hydrogen bonded to the nitrogen. The head-to-tail isomer was

assigned to the more downfield peak, because the hydrogen is between two oxygen, labeled “b.”

The peak labeled “c” is the head-to-head isomer.

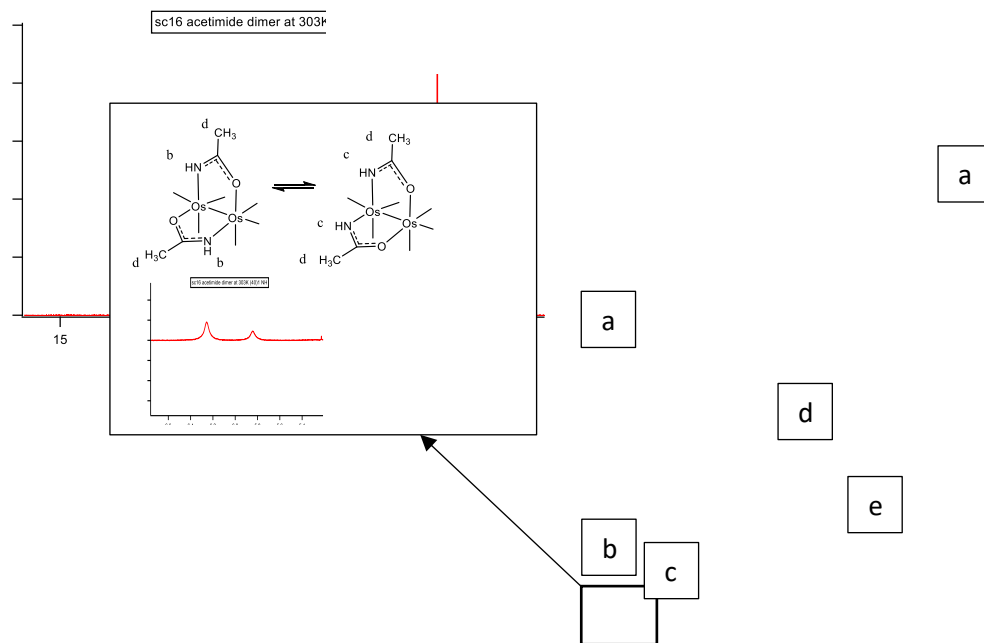
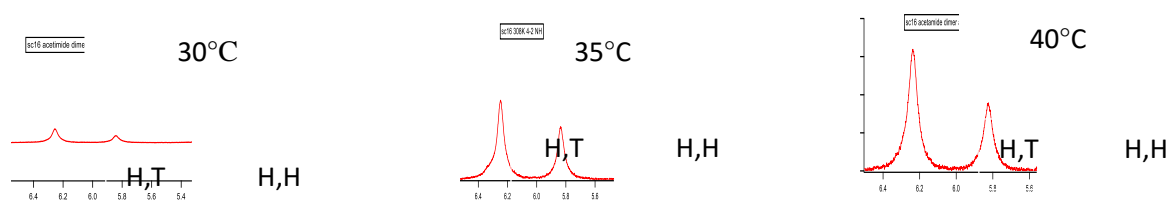


Figure R.12:  $^1\text{H}$  NMR of Isomers B after refluxing at  $110^\circ\text{C}$  (measurement at 303K)

Peaks a are solvent peaks. Peaks e are impurities, because, the product was not dry before dissolving it in  $\text{CDCl}_3$ . However, peaks b and c are the isomers of the hydrogen on the nitrogen. Peak d is a doublet from the hydrogens on the methyl group.

Initially the isomer ratio reflected the temperature of  $110^\circ\text{C}$  (48:52), the isomers were then held at room temperature for some time with sequential  $^1\text{H}$ -NMR scans monitoring until a consistent ratio was seen. A sample of the  $^1\text{H}$ -NMR data can be seen in Figure R.13. The ratios of the isomers were then determined as temperature increased for, 303K, 308K, and 313K . These temperatures were selected to not exceed the boiling point of  $\text{CDCl}_3$ . As the temperature increases the head-to-tail peak increases relative to head-to-head.





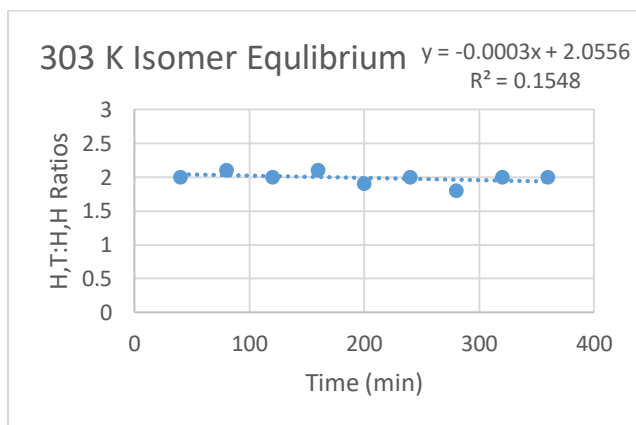
Ratio Average 1.98

2.18

2.26

Figure R.13: Hydrogen on the nitrogen as temperature for the acetamide dimers as the temperature increases the head-tail dimer increases.

Multiple scans were taken to ensure that the isomers were at equilibrium. This data was collected and plotted, in Figure R.13, to determine the equilibrium. Once the the slope of the line is almost zero, we conclude the solution has reached equilibrium.



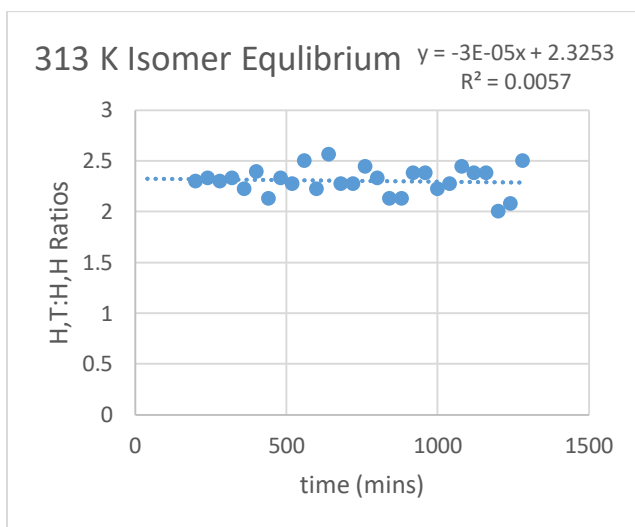
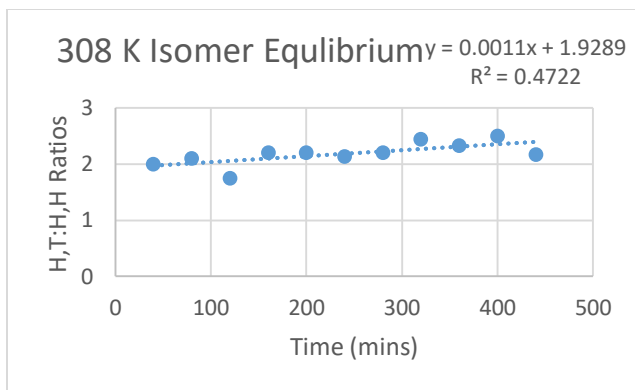


Figure R.13: Head-to-Tail vs Head-to-Head Ratios Reaching Equilibrium series one is data from 303K. Series two is data from 308K. Series three is data from 313K.

The averages were collected at each temperature and calculated to graph a  $\ln(\text{ratio})$  versus  $1/\text{temperature}$ .

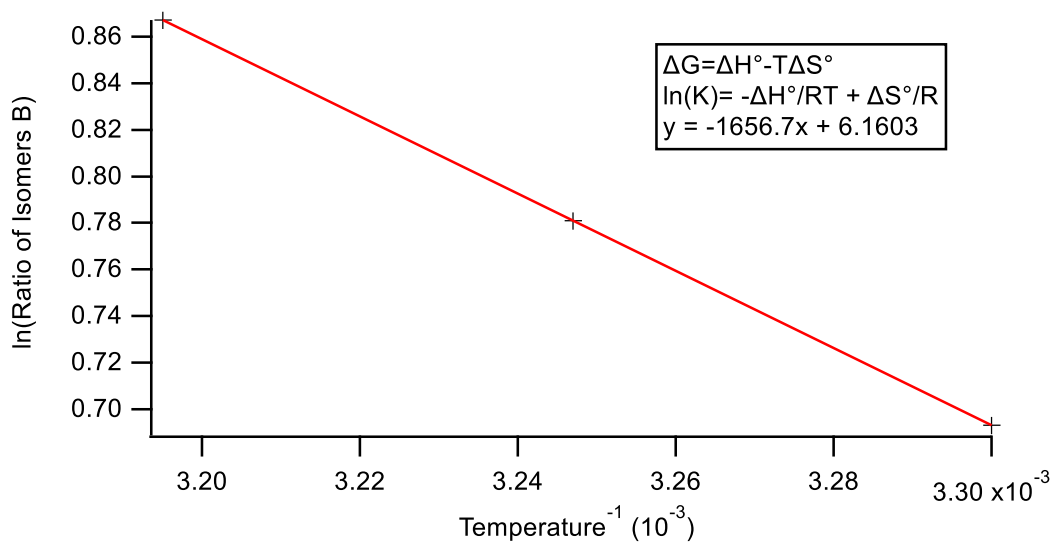


Figure R.15: The natural log of proportion of H,T to H,H vs 1/temperature

The <sup>1</sup>H-NMR results showed the head-to-tail isomer increases as temperature increases. These results are consistent with the thermodynamic product increasing in favorability as temperature increases. In addition to confirming the thermodynamic product, the results gave us the  $\Delta H$  and  $\Delta S$  of the product.  $\Delta H$  is -1.650 kJ; thus, the exchange of the CO ligands to a more polar trans ligand is a favorable process.  $\Delta S$  is +6.14 J/mol; thus, the isomerization to the head-to-tail dimer is spontaneous. In addition, with  $\Delta H$  and  $\Delta S$  values,  $\Delta G$  is known for any temperature.

### Reaction of Isomers with Free Carboxylic acid

The investigation continued by attempting to exchange the coordinated amide of Isomers B with free carboxylic acid in solution. After 2 to 3 hours at 110°C a solution of isomer B and excess carboxylic acid no change in IR spectrum was observed, Figure R.16.

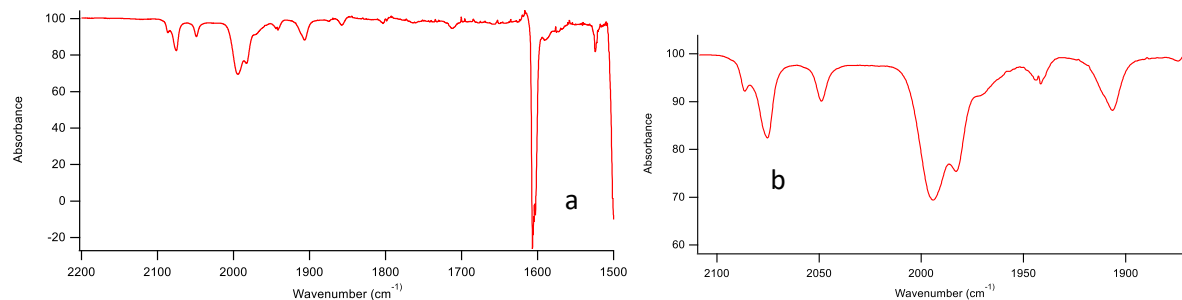


Figure R.16: Isomers B and carboxylic acid reaction mixture.

The left is a spectrum with carboxylic acid peak and the right is zoomed in. The peak labeled “a” are glacial acetic acid in solution and the “b” peak is the polymer. The IR spectrum was taken in  $\text{CH}_2\text{Cl}_2$ :  $2087.9\text{ cm}^{-1}$ ,  $2070.9\text{ cm}^{-1}$ ,  $2050.1\text{ cm}^{-1}$ ,  $1991.8\text{ cm}^{-1}$ , and  $1972\text{ cm}^{-1}$ .

IR and TLC indicate that only the Isomers B are present along with unreacted acetic acid. Thus, the bridged amide does not exchange with carboxylic acid and is strongly bonded to the osmium. This suggests isomerization occurs via an intra-molecular reaction, as hypothesized in Figure R.17. Additionally, the intra-molecular reaction rate is faster and requires less energy than an exchange of the coordinated amide.

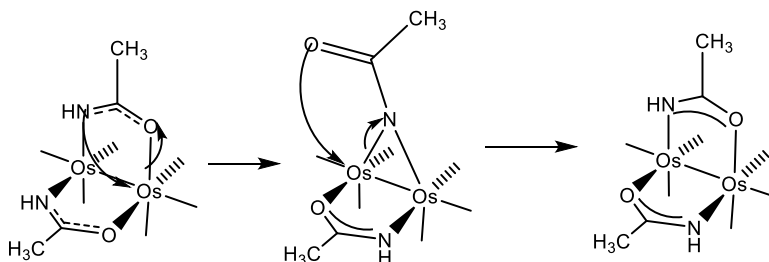


Figure R.17: Hypothesized Intra-conversion

### Alternative Routes to Synthesize Isomer C

As described in the introduction, Powell et al repeated many experiments with triosmiumdodecacarbonyl with carboxylic acid using microwave synthesis, my focus shifted to finding an efficient way to synthesize diosmium diamide product.<sup>15</sup> The reason we followed in Powell’s footsteps and used a microwave as a reaction aid was to eliminate steps and shorten the reaction time. Powell found a large range of products  $\text{Os}_2(\text{CO})_6(\text{RCOO})_2$  with higher yields

could be synthesized when using the microwave. However, in the analogous reaction with benzamide the reaction produced 5 products as seen in the IR and TLC in Figure R.18.

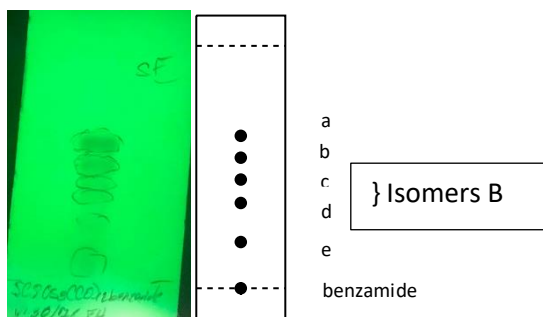
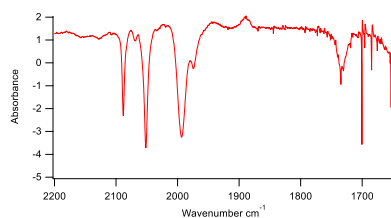


Figure 18: TLC of the microwave reaction mixture.

As a minor product Isomers C were formed corresponding to spots c and d on the TLC and the IR can be seen in Figure 19. The major product has a unique IR band pattern that is an unknown product (Figure R.20). This compound was characterized but no further investigation was carried out.



a

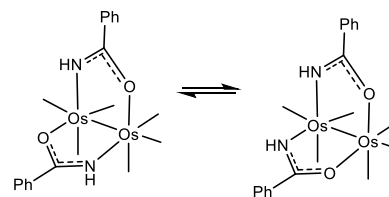


Figure R.19: Isomers C reaction mixture ks labeled "a" at  $1705.4\text{ cm}^{-1}$  and  $1677.6\text{ cm}^{-1}$  are acetamide in solution. The IR spectrum was taken in  $\text{CH}_2\text{Cl}_2$ :  $2087.9\text{ cm}^{-1}$ ,  $2050.1\text{ cm}^{-1}$ ,  $1991.8\text{ cm}^{-1}$ , and  $1972\text{ cm}^{-1}$ .

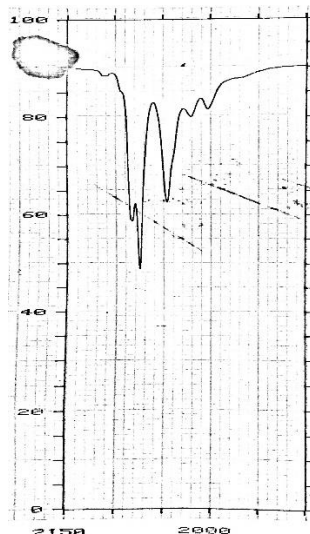
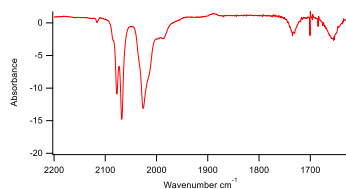


Figure R.20: Major product of microwave reaction with  $Os_3(CO)_{12}$ . Unknown major product of the microwave reaction. The IR peaks of the major product in  $CH_2Cl_2$ :  $2077.5\text{ cm}^{-1}$ ,  $2067.9\text{ cm}^{-1}$ , and  $2025.9\text{ cm}^{-1}$ . Compared to the known  $H_2Os_6(CO)_{18}$  with peaks at  $2081\text{ cm}^{-1}$ ,  $2074\text{ cm}^{-1}$ ,  $2045\text{ cm}^{-1}$ ,  $2020\text{ cm}^{-1}$ , and  $2002\text{ cm}^{-1}$ .

The IR band pattern and frequency is similar to that of  $H_2Os_6(CO)_{18}$  however, the color was yellow not the known a range color of  $H_2Os_6(CO)_{18}$  (Figure R.18).

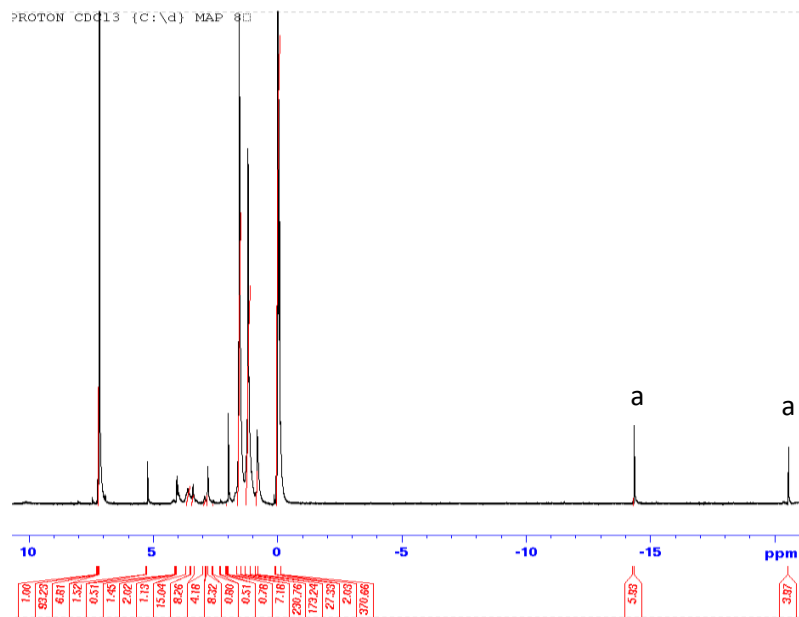


Figure R.21: Major product of microwave reaction with  $Os_3(CO)_{12}$  Peaks labeled "a" are assumed to be bridging hydride ligands

As seen in Figure 21,  $^1\text{H}$  NMR data of the major product indicates that this cluster compound contains two metal hydride at -14 and -20 ppm. Also there are no peaks around 7 ppm correlating to a phenyl group. Triosmiumdodecacarbonyl did not react with the benzamide to give the diosmium diamide as a major product. However, the major product should be further investigated. Overall, using a microwave is not an effective method of synthesis for the diosmium diamide structure. Also confirming that the Pearsall lab's method of synthesizing the diosmium diamide product is the most efficient method.

This same method was used to test Compound A and benzamide in the microwave led to the diosmium dibenzamide product; however, in poor yield.

#### *Notes on Synthesis of $\text{Os}_2(\text{CO})_6(\text{COOR})_2$ Intermediate*

This reaction was designed as an experimental method to isolate the intermediate  $\text{Os}_3(\text{CO})_6(\text{COOR})(\text{OEt})$ , Figure 22, by adding CO (g) to stunt the formation of product of  $\text{Os}_2(\text{CO})_{10}(\text{COOR})_2$ .

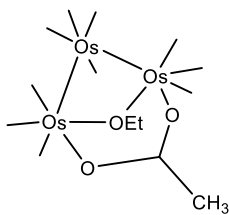


*Figure R.22: intermediate species of  $\text{Os}_2(\text{CO})_6(\text{COOR})_2$*

This product has been synthesized before under low temperature reflux. However, the reaction with Compound A and acetic acid under reflux in toluene at  $110^\circ\text{C}$  resulted in the disappearance of the acetic acid as confirmed by IR. The IR contained only Compound A in solution. The reaction flask started as a light yellow solution and ended as a light yellow solution with an additional white solid around the round bottom glass. This is preliminary data and no further

analysis was done on this reaction, but we assume that this was a catalytic reaction which converted the carboxylic acid to an unknown product, Figure 23.

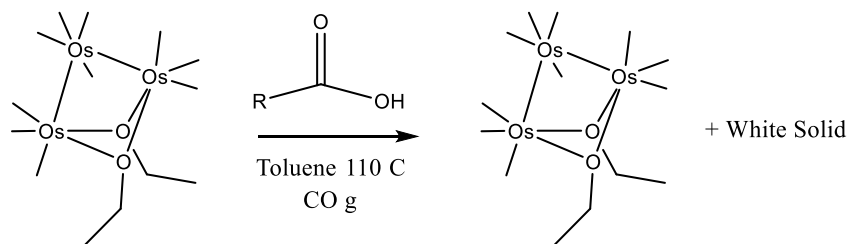


Figure R.23: The reaction mixture of the proposed catalytic reaction with Compound A.

When this reaction was done with acetamide no reaction progressed, with both Compound A and acetamide in solution, allowing a confirmation of the balanced net ionic equation for the synthesis of diosmium diamide product, as seen in Figure 24.

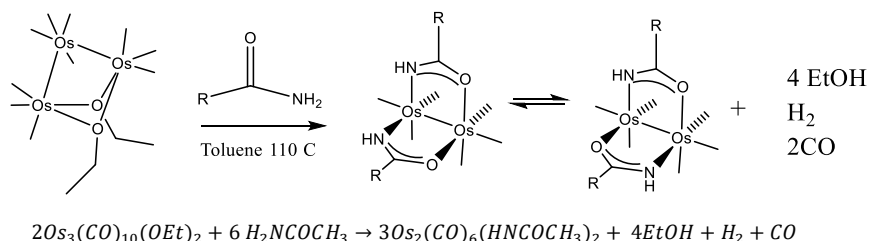


Figure R.24: Balanced equation for the synthesis of diosmium diamide product

## Conclusion

Based on the analysis of data presented in this research paper, we propose an intra-molecular conversion of Isomers B, cis-(H,H) and (H,T), enthalpy and entropy values,  $\Delta S + 6.14$  J and  $\Delta H - 1.65$  kJ. Respectively the intra-molecular conversion was confirmed because there was no exchange of the coordinated acetamide of Isomers B and free acetic acid. Compound D was proposed to be an acetamide polymer structure,  $[\text{Os}_2(\text{CO})_4(\text{CH}_3\text{CONH})_2]_n$ , is bonded together by a weak osmium oxygen bond. In the presence of carbon monoxide, the polymer converted back to the monomer species, Isomers B, as confirmed by IR. When Complex D was



dissolved in acetonitrile the Os-O bonds were replaced as determined by DFT vibration calculations which corresponded to experimental IR spectra. Isomers C did not polymerize, however, prolonged heating of the  $\text{Os}_2(\text{CO})_6(\text{COOCH}_3)_2$  complex lead to a polymer formation, which decomposed to the monomer species over time. In preliminary investigation we demonstrated  $\text{Os}_2(\text{CO})_{10}(\text{OEt})_2$  catalyzes the reactions of acetic acid in an unknown process.

## References-

1. Housecroft; Sharpe, *Inorganic Chemistry*. 4th, Ed. Pearson: Prentice Hall, 2012.
2. Miessler, G.; Tarr, D., *Inorganic Chemistry*. 4th ed.; Pearson: Prentice Hall, 2011.
3. Crabtree, R., *The organometallic chemistry of the transition metals*. 4th ed.; A John Wiley & Sons, Inc.: Yale University, 2005.
4. Buil, M. L.; Esteruelas, M. A.; Gay, M. P.; Gómez-Gallego, M.; Nicasio, A. I.; Oñate, E.; Santiago, A.; Sierra, M. A., Osmium Catalysts for Acceptorless and Base-Free Dehydrogenation of Alcohols and Amines: Unusual Coordination Modes of a BPI Anion. *Organometallics* **2018**, *37* (4), 603-617.
5. Puga, J.; Sánchez-Delgado, R. A.; Ascanio, J.; Braga, D., Conversion of a nitrile ligand into an amido group on a cluster surface; X-ray characterisation of  $[\text{HOs}_4(\text{CO})_{12}\{\mu_3\text{-N}(\text{CO})\text{Me}\}\text{MPPh}_3](\text{M} = \text{Au or Cu})$ . *Journal of the Chemical Society, Chemical Communications* **1986**, (22), 1631-1633.
6. Drover, M. W.; Schafer, L. L.; Love, J. A., Amidate-Ligated Complexes of Rhodium(I): A Showcase of Coordination Flexibility. *Organometallics* **2015**, *34* (10), 1783-1786.
7. Berg, J.; Tymoczko, J.; Gatto, G.; Lubert, S., *Biochemistry*. 8th ed.; W. H. Freeman & Company: 2015.
8. Barragán, F.; Carrion-Salip, D.; Gómez-Pinto, I.; González-Cantó, A.; Sadler, P. J.; de Llorens, R.; Moreno, V.; González, C.; Massaguer, A.; Marchán, V., Somatostatin Subtype-2 Receptor-Targeted Metal-Based Anticancer Complexes. *Bioconjugate Chemistry* **2012**, *23* (9), 1838-1855.
9. Ronconi, L.; Sadler, P. J., Using coordination chemistry to design new medicines. *Coordination Chemistry Reviews* **2007**, *251* (13), 1633-1648.
10. Kong, K. V.; Leong, W. K.; Ng, S. P.; Nguyen, T. H.; Lim, L. H. K., Osmium Carbonyl Clusters: A New Class of Apoptosis Inducing Agents. *ChemMedChem* **2008**, *3* (8), 1269-1275.
11. Burya, S. J.; Palmer, A. M.; Gallucci, J. C.; Turro, C., Photoinduced Ligand Exchange and Covalent DNA Binding by Two New Dirhodium Bis-Amidato Complexes. *Inorganic Chemistry* **2012**, *51* (21), 11882-11890.
12. Burgess, K., Reactions of triosmium clusters with organic compounds. *Polyhedron* **1984**, *3* (11), 1175-1225.
13. Katherine, M. Some Reactions of Triosmium Decacarbonyl Bisethoxide,  $\text{Os}_3(\text{CO})_{10}(\mu^2\text{-OEt})_2$ , with Amides. Drew University, 2017.
14. Lewis J.J., C. G. R., Williams I.G., Chemistry of Polynuclear Compounds Part XVII. Some Carboxylate Complexes of Ruthenium and Osmium Carbonyls. *J.Chem. Soc.* **1969**, 2761-2766.
15. Pyper, K. J.; Jung, J. Y.; Newton, B. S.; Nesterov, V. N.; Powell, G. L., Reactions of  $\text{Os}_3(\text{CO})_{12}$  with carboxylic acids in a microwave reactor; synthesis of  $\text{Os}_2(\text{benzoate})_2(\text{CO})_6$ , a dinuclear osmium(I) compound with aromatic carboxylate ligands. *Journal of Organometallic Chemistry* **2013**, *723*, 103-107.
16. Ainscough, E. W.; Brodie, A. M.; Coll, R. K.; Coombridge, B. A.; Waters, J. M., The reaction of  $[\text{Os}_3(\text{CO})_{10}(\text{CH}_3\text{CN})_2]$  with carboxylic acids: the crystal and molecular structures of  $[\text{Os}_3\text{H}(\text{CO})_{10}(\text{C}_6\text{H}_4(\text{OH})\text{CO}_2)]$  and  $[\text{Os}_3\text{H}(\text{CO})_{10}(\text{C}_6\text{H}_5\text{COS})]$ . *Journal of Organometallic Chemistry* **1998**, *556* (1), 197-205.
17. Shari, D., Ask Dr. Pearsall. Drew University: 1991.
18. Lynn, S., Steric Effects in the Reactions of  $\text{Os}_3(\text{CO})_{10}(\mu^2\text{-OCH}_2\text{CH}_3)_2$  with Carboxylic Acids. Drew University: 2013.
19. Odiaka, T. I., New triosmium metal clusters derived from the reactions between  $[\text{Os}_3(\text{CO})_{10}(\text{NCMe})_2]$  and amides. *Journal of Organometallic Chemistry* **1985**, *284* (1), 95-99.
20. Neumann, F.; Suess-Fink, G., Binuclear ruthenium clusters with nitrogen and oxygen-containing chelate bridges: conversion of  $\mu_2\text{-}\eta_2\text{-pyrazolate}$  ligands into  $\mu_1\text{-}\eta_1\text{-pyrazole}$  ligands by reactions with carboxylic acids. *J. Organomet. Chem.* **1989**, *367* (1-2), 175-85.
21. Hohenberg, P.; Kohn, W., Inhomogeneous Electron Gas. *Physical Review* **1964**, *136* (3B), B864-B871.
22. Bergner, A.; Dolg, M.; Küchle, W.; Stoll, H.; Preuß, H., Ab initio energy-adjusted pseudopotentials for elements of groups 13–17. *Molecular Physics* **1993**, *80* (6), 1431-1441.
23. Leadbeater, N. E., 9.10 Organic Synthesis Using Microwave Heating. In *Comprehensive Organic Synthesis II (Second Edition)*, Knochel, P., Ed. Elsevier: Amsterdam, 2014; pp 234-286.